Mathematical description of a method for deriving XYZ tristimulus spaces

Article · October 1999

CITATIONS
2

READS
335

2 authors:

Jan Henrik Wold
University of South-Eastern Norway
11 PUBLICATIONS **44** CITATIONS
SEE PROFILE

Arne Valberg
Norwegian University of Science and Technology
88 PUBLICATIONS **3,269** CITATIONS
SEE PROFILE

Mathematical description of a method for deriving an *XYZ* tristimulus space

Jan Henrik Wold[1] and Arne Valberg[2]

[1] Department of Physics, University of Oslo, P.O. Box 1048 Blindern, N-0316 Oslo, Norway

[2] Department of Physics, Norwegian University of Science and Technology, N-7491 Trondheim, Norway

UIO/PHYS/99-05 **Received: 1999-10-20**
ISSN-0332-5571

ABSTRACT

This document is a mathematically extended version of the paper “General method for deriving an *XYZ* tristimulus space exemplified by use of the Stiles-Burch$_{1955}$ 2° color matching data” published in “Journal of the Optical Society of America A”, December 1999.

Using, as an example, the color-matching functions of the Stiles-Burch$_{1955}$ 2° pilot group, we give a detailed account of how an *XYZ* representation of tristimulus space can be developed from a given set of color-matching data. Specifically, we present a set of criteria that unequivocally defines the representation. The method outlined is general and can be applied to any set of color-matching data, in particular those sets that are related to the physiological fundamentals.

Key words: colorimetry, *XYZ* representation, tristimulus space, chromaticity diagram.

CONTENTS

1. INTRODUCTION

Commission Internationale de l'Eclairage (CIE) has for some time been active in an attempt to develop a new physiologically based system for colorimetry.[1] This attempt rests on the idea that there exists a linear relationship between color-matching functions (CMF's) and the fundamental response curves of three types of photoreceptor mechanisms — the physiological fundamentals.[2] In this respect, the fundamentals can be regarded as a special representation of CMF's. Psychophysical experiments performed over the past 50 years show that no such connection can be made with satisfactory precision on the basis of the current CIE_{1931} standard colorimetric observer[3,4].

The technical committee CIE TC 1-36 has considered using the Stiles-$Burch_{1959}$ 10° observer[5] (with some minor modifications) as its colorimetric database, because these data represent a body of solid experimental material based exclusively on color matching. With this basis one would like to derive, for the 2° and 10° visual fields, a fundamental tristimulus space accompanied by (1) a chromaticity diagram obtained by a conical projection of the points of this space and (2) an equiluminant chromaticity diagram constructed along the lines of Luther[6] and MacLeod and Boynton[7,8]. However, it is also desirable to establish a connection to the existing CIE_{1931} *XYZ* system, particularly for any set of 2° CMF's that may be derived from the (slightly modified) Stiles-$Burch_{1959}$ 10° observer.[9] Here we will present a general and detailed account of how to design an *XYZ* representation given any set of CMF's. This exercise is useful for two main reasons. First, it has given us the opportunity to review the principles behind the CIE_{1931} colorimetric system. This review has revealed some arbitrariness in the criteria used. Second, since practically all exact color specifications are given in terms of chromaticity coordinates, it would be advantageous to make possible comparisons of chromaticity coordinates of identical stimuli in diagrams that differ minimally.

In the course of this work, we discovered that not all the criteria defining the CIE_{1931} ***XYZ*** tristimulus space were explicitly stated. Some conditions were hard to trace in the literature, and one of these, in particular, was rather loosely formulated. In a recapitulation of the considerations that led to the CIE_{1931} *XYZ* system, we will present the old criteria used by CIE and also introduce some additional constraints to replace the more imprecise original formulations.

In our presentation we will use, as an example, the development of an *XYZ* representation of the CMF's of the Stiles-$Burch_{1955}$ 2° pilot group[10]. We denote this

new representation the $\boldsymbol{X}'\boldsymbol{Y}'\boldsymbol{Z}'$ tristimulus space, and we refer to the corresponding chromaticity diagram as the (x', y') diagram. The diagram has already been used by us in a comparison of the chromaticity differences that result from adopting different sets of physiological fundamentals.[11]

2. THE CIE *XYZ* CONCEPT

A detailed outline of the considerations that led to the current CIE_{1931} *XYZ* system can be found in the paper by Smith and Guild[12] and in the review paper by Fairman *et al.*[13] The well-known main criteria may be listed as follows:

1. All color stimuli are to have all non-negative tristimulus values.
2. In the chromaticity diagram the alychne is to be represented by a line coinciding with the abscissa axis.
3. The chromaticity coordinates of Illuminant *E* (the equal power spectrum) are to equal $\frac{1}{3}$ each.

In principle, there are many ways to ensure that criterion 1 is fulfilled.[14,15] The procedure actually followed in developing the CIE_{1931} standard was to choose the new (virtual) primaries ***X***, ***Y***, and ***Z*** so that, in the chromaticity diagram of the CIE *RGB* (red-green-blue) representation (referring to physical primaries) [16,17], their chromaticity points define the vertices of a triangle that fully circumscribes the spectrum locus.[12]

Criterion 2 requires that two of the primaries be represented on the alychne, with the consequence that the CMF referring to the remaining primary is proportional to the adopted spectral luminous efficiency function.[14,18] In CIE's standard representation this proportionality between the CMF $\bar{y}(\lambda)$ and the CIE spectral luminous efficiency function for photopic vision[19] is restricted to identity — i.e., $\bar{y}(\lambda) \equiv V(\lambda)$.

Criterion 3 implies that the CMF's must be normalized so that their integrals over the spectrum are the same for all three functions.

Obviously, criteria 1-3 do not define a unique *XYZ* representation. In order to unequivocally define the representation, additional constraints are necessary. In the relevant publications these constraints concern the sides of the triangle that circumscribes the spectrum locus in the *RGB* representation. For instance, regarding the boundary connecting the chromaticity points of the primaries ***X*** and ***Y*** — the side *XY* — Smith and Guild stated: [12]

> *"The side XY of the colour triangle* [the circumscribing triangle] *is made to pass through R, the red terminus of the spectral locus…. To extend the number of zero coordinates as far as possible, we make XY tangential to the spectral locus at R."*

Whereas the above criterion is quite precise, the conditions for determining the side *YZ* are less accurate:[12]

> *"The conditions are that it* [side *YZ*] *should pass the spectral locus at a reasonable distance, and lie in a direction which give a favourable disposition of the spectral locus within the triangle."*

3. CONCEPT OF THE NEW $X^{\cdot}Y^{\cdot}Z^{\cdot}$ TRISTIMULUS SPACE

In designing a new colorimetric *XYZ* system, one may discuss which criteria are useful. In deriving an *XYZ* representation of the Stiles-Burch$_{1955}$ 2° pilot group, we have made the decision to apply much the same principles as those used in developing the CIE$_{1931}$ standard, but to state the requirements more precisely whenever necessary. We have preferred an exact mathematical method, based partly on geometrical considerations.

It should be emphasized, however, that this approach is only one of many possible alternatives.

A vital point in our method regards the constraints imposed on the side *YZ* of the circumscribing triangle, in which the Smith-Guild formulation above is replaced by the requirement of minimum difference between the new $(x^{\cdot}, y^{\cdot})$ diagram and our chosen reference diagram[20–22] — the Judd-Vos (x', y') diagram[23,24]. Moreover, on the assumption that the S cone does not contribute to luminance,[25–29] the spectral luminous efficiency function defining the alychne in $\boldsymbol{X^{\cdot}Y^{\cdot}Z^{\cdot}}$ space has been chosen to equal a linear combination of the 2° fundamental L and M response curves (L and M fundamentals) given by Stockman *et al.*[30] We denote this synthesized spectral luminous efficiency function $V^{\cdot}(\lambda)$.

Now, in order to comply with the CIE 1931 procedure, modified as outlined above, we propose that the main steps in developing the new Stiles-Burch$_{1955}$ $\boldsymbol{X^{\cdot}Y^{\cdot}Z^{\cdot}}$ tristimulus space should be as follows:

1. Transform the Judd-Vos (x', y') diagram to an (r', g') diagram that (a) refers to Wright primaries $\boldsymbol{R}'$, $\boldsymbol{G}'$, and $\boldsymbol{B}'$ representing monochromatic stimuli of wavelengths 700.0, 546.1, and 435.8 nm, respectively, and (b) has Illuminant *E* represented at the point $(r'_E, g'_E) = (\frac{1}{3}, \frac{1}{3})$.

2. Transform the original Stiles-Burch$_{1955}$ $(\hat{r}^{\cdot}, \hat{g}^{\cdot})$ diagram (referring to primaries $\hat{\boldsymbol{R}}^{\cdot}$, $\hat{\boldsymbol{G}}^{\cdot}$, and $\hat{\boldsymbol{B}}^{\cdot}$ that represent unit radiance, monochromatic stimuli with wave numbers 15500, 19000, and 22500 cm^{-1}, respectively) into an $(r^{\cdot}, g^{\cdot})$ diagram that (a) refers to Wright primaries $\boldsymbol{R}^{\cdot}$, $\boldsymbol{G}^{\cdot}$, and $\boldsymbol{B}^{\cdot}$ that represent monochromatic stimuli of wavelengths 700.0, 546.1, and 435.8 nm, respectively, and (b) has Illuminant *E* represented at the point $(r_E^{\cdot}, g_E^{\cdot}) = (\frac{1}{3}, \frac{1}{3})$.

3. In the $(r^{\cdot}, g^{\cdot})$ diagram choose the chromaticity points for the new primaries $\boldsymbol{X}^{\cdot}$, $\boldsymbol{Y}^{\cdot}$, and $\boldsymbol{Z}^{\cdot}$ so that the following criteria are fulfilled:

   (i) The chromaticity points of the primaries $\boldsymbol{X}^{\cdot}$, $\boldsymbol{Y}^{\cdot}$, and $\boldsymbol{Z}^{\cdot}$ define the vertices of a triangle that fully circumscribes the spectrum locus.

   (ii) The boundary connecting the chromaticity points of the primaries $\boldsymbol{X}^{\cdot}$ and $\boldsymbol{Z}^{\cdot}$ (the side *XZ*) coincides with the line representing the alychne as defined relative to the synthesized $V^{\cdot}(\lambda)$.

   (iii) The boundary connecting the chromaticity points of the primaries $\boldsymbol{X}^{\cdot}$ and $\boldsymbol{Y}^{\cdot}$ (the side *XY*)

   – has the same slope as the line connecting the chromaticity points of the primaries $\boldsymbol{X}'$ and $\boldsymbol{Y}'$ in the Judd-Vos (r', g') diagram.
   – is tangent to the spectrum locus in the long wavelength region (when the locus is interpolated as outlined in Appendix D).

   (iv) The shortest distance from the spectrum locus to the boundary connecting the chromaticity points of the primaries $\boldsymbol{Y}^{\cdot}$ and $\boldsymbol{Z}^{\cdot}$ (the side *YZ*) is equal to the corresponding distance in the Judd-Vos (r', g') diagram (the loci being interpolated as outlined in Appendix D).

   (v) When the above criteria are obeyed, the mean Euclidean difference between corresponding points on the spectrum loci in the new $(x^{\cdot}, y^{\cdot})$ diagram and the Judd-Vos (x', y') diagram is minimum according to a least-root-mean-square (RMS) criterion, calculated at 1-nm intervals. (This criterion determines the slope of the side *YZ* in the $(r^{\cdot}, g^{\cdot})$ diagram.)

4. From the $r^{\cdot}$ and $g^{\cdot}$ coordinates of the primaries $\boldsymbol{X}^{\cdot}$, $\boldsymbol{Y}^{\cdot}$, and $\boldsymbol{Z}^{\cdot}$, derive a new $(x^{\cdot}, y^{\cdot})$ chromaticity diagram satisfying the criterion

   (vi) Illuminant *E* is represented at the point $(x_E^{\cdot}, y_E^{\cdot}) = (\frac{1}{3}, \frac{1}{3})$.

5. Determine the CMF's $\bar{x}^{\cdot}(\lambda)$, $\bar{y}^{\cdot}(\lambda)$, and $\bar{z}^{\cdot}(\lambda)$ under the constraint
   (vii) $\bar{y}^{\cdot}(\lambda) \equiv V^{\cdot}(\lambda)$.

Criteria (i), (ii), and (vi), parallel CIE criteria 1, 2, and 3, respectively. Furthermore, criteria (iii), (iv), and (v) are those that have been introduced to unequivocally define the representation, thereby replacing the more imprecise formulations of Smith and Guild[12].

The remaining criterion, (vii), ensures that the final representation is in conformity with CIE's standard by requiring that the choice of a common scaling factor for the CMF's makes the CMF that refers to the *Y* primary identical to the adopted spectral luminous efficiency function.

4. (r', g') CHROMATICITY DIAGRAM OF THE JUDD-VOS MODIFIED 2° OBSERVER

Since the Judd-Vos modified 2° observer[23,24] is considered a significant improvement of the CIE_{1931} standard colorimetric observer[3,4], we decided to use the Judd-Vos (x', y') chromaticity diagram as a reference in our work. Furthermore, in order to follow as closely as possible the procedure adopted by CIE, we regarded it as important to refer all geometric manipulations to a corresponding Judd-Vos (r', g') diagram. This diagram refers to Wright primaries $\boldsymbol{R}'$, $\boldsymbol{G}'$ and $\boldsymbol{B}'$ that represent monochromatic stimuli of wavelengths 700.0, 546.1, and 435.8 nm, respectively, and has Illuminant *E* represented at the point $(r'_E, g'_E) = (\frac{1}{3}, \frac{1}{3})$. Since the Judd-Vos modified 2° observer was obtained by simply adjusting the CIE_{1931} CMF's $\bar{x}(\lambda)$, $\bar{y}(\lambda)$, and $\bar{z}(\lambda)$ directly, without reference back to an *RGB* representation, no such (r', g') diagram was ever published. Being relevant for the work at hand, this diagram therefore had to be derived separately.

For the Judd-Vos modified 2° observer, let

- $\boldsymbol{R}'_j$ $(j = 1, 2, 3)$ denote the primaries $\boldsymbol{R}'$, $\boldsymbol{G}'$, and $\boldsymbol{B}'$ of the *RGB* representation;
- λ_j $(j = 1, 2, 3)$ denote the wavelengths of the monochromatic stimuli represented by the primaries $\boldsymbol{R}'_j$ $(j = 1, 2, 3)$ of the *RGB* representation;
- r'_{jQ} $(j = 1, 2, 3)$ denote the chromaticity coordinates r'_Q, g'_Q, and b'_Q of a stimulus *Q* in *RGB* representation;
- $\bar{x}'_i(\lambda)$ $(i = 1, 2, 3)$ denote the CMF's $\bar{x}'(\lambda)$, $\bar{y}'(\lambda)$, and $\bar{z}'(\lambda)$ in the *XYZ* representation;

– $\bar{x}'_{i\lambda}$ $(i = 1, 2, 3)$ denote the spectral tristimulus values $\bar{x}'_\lambda$, $\bar{y}'_\lambda$, and $\bar{z}'_\lambda$ of a stimulus of wavelength λ in *XYZ* representation;

– x'_{iQ} $(i = 1, 2, 3)$ denote the chromaticity coordinates x'_Q, y'_Q, and z'_Q of a stimulus Q in *XYZ* representation;

– x'_{ij} $(i, j = 1, 2, 3)$ denote the chromaticity coordinates of the primaries $\boldsymbol{R}'_j$ $(j = 1, 2, 3)$ in *XYZ* representation — i.e., $x'_{ij} \equiv x'_{iR'_j}$.

Then, according to Eqs. (A.2) of Appendix A, using Illuminant *E* as a normalization stimulus, the projective transformation $T^{r'}_{x'}$ from the chromaticity coordinates x'_{iQ} $(i = 1, 2, 3)$ to the new chromaticity coordinates r'_{jQ} $(j = 1, 2, 3)$ is

$$T^{r'}_{x'}: \quad r'_{jQ} = \frac{\sum_{i=1}^{3} \mathbb{X}^{R'}_{ij}\, x'_{iQ}}{\sum_{l,i=1}^{3} \mathbb{X}^{R'}_{il}\, x'_{iQ}}\,, \qquad \mathbb{X}^{R'}_{ij} \equiv \frac{r'_{jE}\, \mathbb{X}^{R'}_{ij}}{\sum_{\rho=1}^{3} \mathbb{X}^{R'}_{\rho j}\, x'_{\rho E}} \qquad (j = 1, 2, 3)\,, \tag{1}$$

with the coefficient $\mathbb{X}^{R'}_{ij}$ being the cofactor of element x'_{ij} in the matrix $\left(x'_{ij}\right) \equiv \left(x'_{iR'_j}\right)$. The matrix elements $x'_{ij} \equiv x'_{iR'_j}$ $(i, j = 1, 2, 3)$ — i.e., the chromaticity coordinates of the new primaries $\boldsymbol{R}'_j$ $(j = 1, 2, 3)$ in the original Judd-Vos *XYZ* representation — are given by the equations

$$x'_{ij} = \frac{\bar{x}'_{i\lambda_j}}{\sum_{l=1}^{3} \bar{x}'_{l\lambda_j}} \qquad (i, j = 1, 2, 3)\,. \tag{2}$$

When the spectral tristimulus values $\bar{x}'_{i\lambda}$ $(i = 1, 2, 3)$ are computed by interpolating the CMF's $\bar{x}'_i(\lambda)$ $(i = 1, 2, 3)$[24] as outlined in Appendix D, the following coordinate values are determined:

$$\begin{aligned}
&x'_{11} \equiv x'_{R'} = 0.730100\,, \quad x'_{21} \equiv y'_{R'} = 0.269857\,, \quad x'_{31} \equiv z'_{R'} = 0.000043\,,\\
&x'_{12} \equiv x'_{G'} = 0.275117\,, \quad x'_{22} \equiv y'_{G'} = 0.716046\,, \quad x'_{32} \equiv z'_{G'} = 0.008837\,,\\
&x'_{13} \equiv x'_{B'} = 0.169856\,, \quad x'_{23} \equiv y'_{B'} = 0.017098\,, \quad x'_{33} \equiv z'_{B'} = 0.813046\,.
\end{aligned} \tag{3}$$

In the Judd-Vos *XYZ* representation, the (x', y') diagram deviates from ideality in having the chromaticity point of Illuminant *E* slightly displaced from the ideal point $(\frac{1}{3}, \frac{1}{3})$. According to Vos' tabulations[24,31] the chromaticity coordinates of *E* are

$$x'_{1E} \equiv x'_E = 0.33499\,, \qquad x'_{2E} \equiv y'_E = 0.33618\,, \qquad x'_{3E} \equiv z'_E = 0.32883\,. \tag{4}$$

Regarding the new *RGB* representation, we are allowed to choose the chromaticity coordinates of Illuminant *E* freely (within the above restrictions). Thus, we make the representation ideal by placing its chromaticity point at exactly $(\frac{1}{3},\ \frac{1}{3})$ in the new $(r',\, g')$ diagram, that is

$$r'_{1E} \equiv r'_E = \tfrac{1}{3}\,, \qquad r'_{2E} \equiv g'_E = \tfrac{1}{3}\,, \qquad r'_{3E} \equiv b'_E = \tfrac{1}{3}\,. \tag{5}$$

Now, determining the coefficients $\mathbb{X}_{ij}^{R'}$ $(i, j = 1, 2, 3)$ in the transformation $T_{x'}^{r'}$ [Eqs. (1)] by means of the matrix elements x'_{ij} $(i, j = 1, 2, 3)$ [Eqs. (2)], inserting the values of the chromaticity coordinates x'_{iE} $(i = 1, 2, 3)$ and r'_{jE} $(j = 1, 2, 3)$ [Eqs. (3) and (4)], and ultimately eliminating the coordinate $x'_{3Q} \equiv z'_Q$ using the relation $z'_Q = 1 - x'_Q - y'_Q$, the equations transforming the chromaticity coordinates x'_Q and y'_Q into new coordinates r'_Q and g'_Q read

$$\begin{aligned} r'_Q &= \frac{4.532604\, x'_Q - 0.682602\, y'_Q - 0.758220}{1.933206\, x'_Q - 0.165284\, y'_Q + 1}\,, \\ g'_Q &= \frac{-0.978903\, x'_Q + 2.169755\, y'_Q + 0.129175}{1.933206\, x'_Q - 0.165284\, y'_Q + 1}\,. \end{aligned} \tag{6}$$

With $\boldsymbol{X}'$, $\boldsymbol{Y}'$, and $\boldsymbol{Z}'$ being the primaries of the *XYZ* representation, their chromaticity points in the (x', y') diagram will necessarily be $(x'_{X'}, y'_{X'}) = (1,\ 0)$, $(x'_{Y'}, y'_{Y'}) = (0,\ 1)$, and $(x'_{Z'}, y'_{Z'}) = (0,\ 0)$. When applying the above transformation, the chromaticity coordinates of $\boldsymbol{X}'$, $\boldsymbol{Y}'$, and $\boldsymbol{Z}'$ in the new *RGB* representation turn out to be

$$\begin{aligned} &r'_{X'} = 1.286778\,, \quad g'_{X'} = -0.289693\,, \quad b'_{X'} = 1 - r'_{X'} - g'_{X'} = 0.002915\,, \\ &r'_{Y'} = -1.726122\,, \quad g'_{Y'} = 2.754146\,, \quad b'_{Y'} = 1 - r'_{Y'} - g'_{Y'} = -0.028024\,, \\ &r'_{Z'} = -0.758220\,, \quad g'_{Z'} = 0.129175\,, \quad b'_{Z'} = 1 - r'_{Z'} - g'_{Z'} = 1.629045\,. \end{aligned} \tag{7}$$

Figure 1A shows the original Judd-Vos (x', y') diagram, and Fig. 1B shows the new (r', g') diagram. Both diagrams show (1) the chromaticity points (X'), (Y'), and (Z') of the original primaries $\boldsymbol{X}'$, $\boldsymbol{Y}'$, and $\boldsymbol{Z}'$; (2) the chromaticity points (R'), (G'), and (B') of the new primaries $\boldsymbol{R}'$, $\boldsymbol{G}'$, and $\boldsymbol{B}'$ and (3) the chromaticity point (E) of Illuminant *E*. Also drawn in Fig. 1B are the straight lines L'_1, L'_2, and L'_3

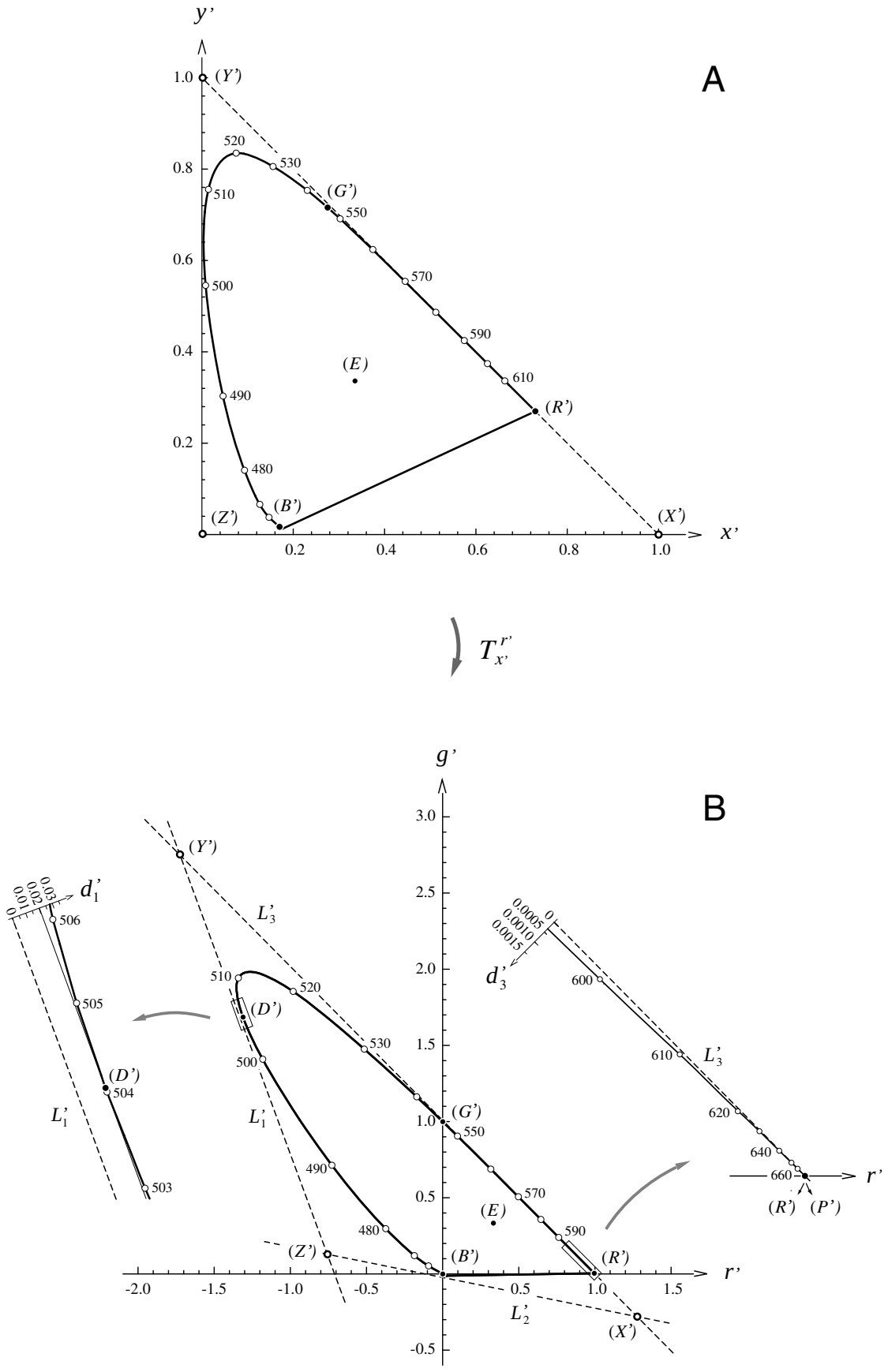
A
y'
x'
(Y')
(G')
(E)
(R')
(B')
(Z')
(X')
520
530
510
550
570
500
590
610
490
480
1.0
0.8
0.6
0.4
0.2
0.2
0.4
0.6
0.8
1.0
$T_{x'}^{r'}$
B
g'
r'
d_1'
d_3'
L_1'
L_2'
L_3'
(D')
(P')
506
505
504
503
600
620
640
660
3.0
2.5
2.0
1.5
1.0
0.5
-0.5
-2.0
-1.5
-1.0
-0.5
0.5
1.0
1.5

Figure 1

connecting the chromaticity points (X'), (Y'), and (Z') of the old primaries $\boldsymbol{X}'$, $\boldsymbol{Y}'$, and $\boldsymbol{Z}'$. The inset diagrams to the left and right show magnifications of the two locus segments framed in the main plot. The ordinates d_1' and d_3' of these blowups give the Euclidean distances between the points on the locus segments and their respective closest points on the lines L_1' and L_3' (the spectrum locus being interpolated as outlined in Appendix D).

Numerical analysis shows that the distance $d_{1D'}'$ between L_1' — the *YZ* side of the circumscribing triangle — and the locus point (D') closest to the line is

$$d_{1D'}' = 0.020365. \tag{8}$$

The parameter value at (D') turns out to be $\lambda_{D'} = 504.046$ nm, and accordingly, (D') is given as $(r_{D'}', g_{D'}') = (-1.308762, 1.681121)$.

Regarding the line L_3' connecting the points (X') and (Y') — the *XY* side of the circumscribing triangle — its slope α_3' is

$$\alpha_3' = \frac{g_{Y'}' - g_{X'}'}{r_{Y'}' - r_{X'}'} = -1.010269. \tag{9}$$

In our development of an *XYZ* representation of the Stiles-Burch$_{1955}$ 2° pilot group, the parameters $d_{1D'}'$ and α_3' play a central role in that their values are adopted for the corresponding parameters that unequivocally determine the chromaticity coordinates of the new primaries $\boldsymbol{X}^{\cdot}$, $\boldsymbol{Y}^{\cdot}$, and $\boldsymbol{Z}^{\cdot}$ in a diagram analogous to the (r', g') diagram of Fig. 1B.

Figure 1 **A**: (x', y') chromaticity diagram of the Judd-Vos modified 2° observer. Filled circles on the spectrum locus mark the chromaticity points (R'), (G'), and (B') of the new Wright primaries. The chromaticity point (*E*) of Illuminant *E* is positioned at $(x_E', y_E') = (0.33499, 0.33618)$, i.e., slightly displaced from the ideal point $(\frac{1}{3}, \frac{1}{3})$. **B**: (r', g') chromaticity diagram of the Judd-Vos modified 2° observer resulting from transformation $T_{x'}^{r'}$ [Eqs. (6)]. The diagram refers to Wright primaries $\boldsymbol{R}'$, $\boldsymbol{G}'$, and $\boldsymbol{B}'$ representing monochromatic stimuli of wavelengths 700.0, 546.1, and 435.8 nm, normalized so that the chromaticity point (*E*) of Illuminant *E* is positioned at $(r_E', g_E') = (\frac{1}{3}, \frac{1}{3})$. Lines L_1', L_2', and L_3' (dashed) constitute a circumscribing triangle with vertices at the chromaticity points (X'), (Y'), and (Z') of the old primaries. Ordinates d_1' and d_3' of the inset magnifications give the Euclidean distances between the points on the locus segments (framed) and their respective closest points on the lines L_1' and L_3'. Point (D') marks the locus point of shortest distance to line L_1'. Line L_3' intersects the abscissa axis in point (P').

5. $(r^{\cdot}, g^{\cdot})$ CHROMATICITY DIAGRAM OF THE STILES-BURCH$_{1955}$ 2° PILOT GROUP

The original tabulations of the Stiles-Burch$_{1955}$ 2° pilot group[10,31] are given in an $\hat{R}\hat{G}\hat{B}$ representation, referring to primaries $\hat{\boldsymbol{R}}^{\cdot}$, $\hat{\boldsymbol{G}}^{\cdot}$, and $\hat{\boldsymbol{B}}^{\cdot}$ that represent monochromatic stimuli of unit radiance and wave numbers 15500, 19000, and 22500 cm^{-1}, respectively. Initially, therefore, in order to develop the *XYZ* representation in compliance with the CIE procedure, we transformed the $(\hat{r}^{\cdot}, \hat{g}^{\cdot})$ diagram of the $\hat{R}\hat{G}\hat{B}$ representation into an $(r^{\cdot}, g^{\cdot})$ diagram analogous to the (r, g) diagram in the *RGB* representation of the CIE$_{1931}$ standard colorimetric observer. In doing this, much the same steps were followed as in the derivation of the Judd-Vos (r', g') diagram.

For the Stiles-Burch$_{1955}$ 2° pilot group, let

- $\boldsymbol{R}_j^{\cdot}$ $(j = 1, 2, 3)$ denote the primaries $\boldsymbol{R}^{\cdot}$, $\boldsymbol{G}^{\cdot}$, and $\boldsymbol{B}^{\cdot}$ of the *RGB* representation;
- λ_j $(j = 1, 2, 3)$ denote the wavelengths of the monochromatic stimuli represented by the primaries $\boldsymbol{R}_j^{\cdot}$ $(j = 1, 2, 3)$ of the *RGB* representation;
- $r_{jQ}^{\cdot}$ $(j = 1, 2, 3)$ denote the chromaticity coordinates $r_Q^{\cdot}$, $g_Q^{\cdot}$, and $b_Q^{\cdot}$ of a stimulus Q in *RGB* representation;
- $\bar{\hat{r}}_i^{\cdot}(\lambda)$ $(i = 1, 2, 3)$ denote the CMF's $\bar{\hat{r}}^{\cdot}(\lambda)$, $\bar{\hat{g}}^{\cdot}(\lambda)$, and $\bar{\hat{b}}^{\cdot}(\lambda)$ in the $\hat{R}\hat{G}\hat{B}$ representation;
- $\bar{\hat{r}}_{i\lambda}^{\cdot}$ $(i = 1, 2, 3)$ denote the spectral tristimulus values $\bar{\hat{r}}_{\lambda}^{\cdot}$, $\bar{\hat{g}}_{\lambda}^{\cdot}$, and $\bar{\hat{b}}_{\lambda}^{\cdot}$ of a stimulus of wavelength λ in $\hat{R}\hat{G}\hat{B}$ representation;
- $\hat{r}_{iQ}^{\cdot}$ $(i = 1, 2, 3)$ denote the chromaticity coordinates $\hat{r}_Q^{\cdot}$, $\hat{g}_Q^{\cdot}$, and $\hat{b}_Q^{\cdot}$ of a stimulus Q in $\hat{R}\hat{G}\hat{B}$ representation;
- $\hat{r}_{ij}^{\cdot}$ $(i, j = 1, 2, 3)$ denote the chromaticity coordinates of the primaries $\boldsymbol{R}_j^{\cdot}$ $(j = 1, 2, 3)$ in $\hat{R}\hat{G}\hat{B}$ representation — i.e., $\hat{r}_{ij}^{\cdot} \equiv \hat{r}_{iR_j}^{\cdot}$.

Then, it follows from Eqs. (A.2) of Appendix A, that by using Illuminant *E* as normalization stimulus, the projective transformation from the original chromaticity coordinates $\hat{r}_{iQ}^{\cdot}$ $(i = 1, 2, 3)$ to chromaticity coordinates $r_{jQ}^{\cdot}$ $(j = 1, 2, 3)$ is

$$T_{\hat{r}^{\cdot}}^{r^{\cdot}}: \qquad r_{jQ}^{\cdot} = \frac{\sum_{i=1}^{3} \hat{\mathbb{R}}_{ij}^{R^{\cdot}} \, \hat{r}_{iQ}^{\cdot}}{\sum_{l,i=1}^{3} \hat{\mathbb{R}}_{il}^{R^{\cdot}} \, \hat{r}_{iQ}^{\cdot}} \,, \qquad \hat{\mathbb{R}}_{ij}^{R^{\cdot}} \equiv \frac{r_{jE}^{\cdot} \, \hat{r}_{ij}^{R^{\cdot}}}{\sum_{\rho=1}^{3} \hat{r}_{\rho j}^{R^{\cdot}} \, \hat{r}_{\rho E}^{\cdot}} \qquad (j = 1, 2, 3) \,, \qquad (10)$$

with the coefficient $\hat{\mathcal{F}}_{ij}^{R\cdot}$ being the cofactor of element $\hat{r}_{ij}^{\cdot}$ in the matrix $\left(\hat{r}_{ij}^{\cdot}\right) \equiv \left(\hat{r}_{iR_j}^{\cdot}\right)$. The matrix elements $\hat{r}_{ij}^{\cdot} \equiv \hat{r}_{iR_j}^{\cdot}$ $(i, j = 1, 2, 3)$ — i.e. the chromaticity coordinates of the new primaries $\boldsymbol{R}_j^{\cdot}$ $(j = 1, 2, 3)$ in the original Stiles-Burch $\hat{R}\hat{G}\hat{B}$ representation — are given by the equations

$$\hat{r}_{ij}^{\cdot} = \frac{\bar{\hat{r}}_{i\lambda_j}^{\cdot}}{\sum_{l=1}^{3} \bar{\hat{r}}_{l\lambda_j}^{\cdot}} \qquad (i, j = 1, 2, 3) \ . \tag{11}$$

When the spectral tristimulus values are computed by interpolating the 1-nm tabulations of the CMF's $\bar{\hat{r}}_i^{\cdot}(\lambda)$ $(i = 1, 2, 3)$[31] in the manner outlined in Appendix D, the following coordinate values are determined:

$$\begin{aligned}
&\hat{r}_{11}^{\cdot} \equiv \hat{r}_{R\cdot}^{\cdot} = 1.008820\,, \qquad \hat{r}_{21}^{\cdot} \equiv \hat{g}_{R\cdot}^{\cdot} = -0.009413\,, \qquad \hat{r}_{31}^{\cdot} \equiv \hat{b}_{R\cdot}^{\cdot} = 0.000593\,, \\
&\hat{r}_{12}^{\cdot} \equiv \hat{r}_{G\cdot}^{\cdot} = 0.379787\,, \qquad \hat{r}_{22}^{\cdot} \equiv \hat{g}_{G\cdot}^{\cdot} = 0.628741\,, \qquad \hat{r}_{32}^{\cdot} \equiv \hat{b}_{G\cdot}^{\cdot} = -0.008528\,, \\
&\hat{r}_{13}^{\cdot} \equiv \hat{r}_{B\cdot}^{\cdot} = 0.032081\,, \qquad \hat{r}_{23}^{\cdot} \equiv \hat{g}_{B\cdot}^{\cdot} = -0.016113\,, \qquad \hat{r}_{33}^{\cdot} \equiv \hat{b}_{B\cdot}^{\cdot} = 0.984032\,.
\end{aligned} \tag{12}$$

In the $\hat{R}\hat{G}\hat{B}$ representation — referring to primaries that represent unit radiance reference stimuli — the chromaticity coordinates of Illuminant *E* are not explicitly given as part of the representation criteria. Thus, the coordinates $\hat{r}_{iE}^{\cdot}$ $(i = 1, 2, 3)$ embodied in the transformation $T_{\hat{r}}^{r\cdot}$ [Eqs. (10)] have to be computed by means of the equations

$$\hat{r}_{iE}^{\cdot} = \frac{\int_{390}^{730} \bar{\hat{r}}_i^{\cdot}(\lambda)\, d\lambda}{\sum_{l=1}^{3} \int_{390}^{730} \bar{\hat{r}}_l^{\cdot}(\lambda)\, d\lambda} \qquad (i = 1, 2, 3) \ . \tag{13}$$

When, in compliance with the CIE recommendations[32,33], the integrands $\bar{\hat{r}}_i^{\cdot}(\lambda)$ $(i = 1, 2, 3)$ are taken as the continuous functions obtained by piecewise third order polynomial interpolation of the Stiles-Burch 1-nm tabulations[31], the values determined are

$$\hat{r}_{1E}^{\cdot} \equiv \hat{r}_{E}^{\cdot} = 0.579468\,, \qquad \hat{r}_{2E}^{\cdot} \equiv \hat{g}_{E}^{\cdot} = 0.265210\,, \qquad \hat{r}_{3E}^{\cdot} \equiv \hat{b}_{E}^{\cdot} = 0.155322\,. \tag{14}$$

In the *RGB* representation of the Stiles-Burch$_{1955}$ 2° pilot group, the chromaticity coordinates of Illuminant *E* are assigned the same values as in the *RGB* representations of the CIE$_{1931}$ standard colorimetric observer and the Judd-Vos modified 2° observer, i.e.,

$$r_{1E}^{\cdot} \equiv r_E^{\cdot} = \tfrac{1}{3}, \qquad r_{2E}^{\cdot} \equiv g_E^{\cdot} = \tfrac{1}{3}, \qquad r_{3E}^{\cdot} \equiv b_E^{\cdot} = \tfrac{1}{3}\ . \tag{15}$$

Calculations analogous to those applied in the derivation of Eqs. (6) now give the following transformation equations from Stiles and Burch's original chromaticity coordinates $\hat{r}_Q^{\cdot}$ and $\hat{g}_Q^{\cdot}$ to the new chromaticity coordinates $r_Q^{\cdot}$ and $g_Q^{\cdot}$:

$$\begin{aligned} r_Q^{\cdot} &= \frac{0.403966\,\hat{r}_Q^{\cdot} - 0.217818\,\hat{g}_Q^{\cdot} - 0.016470}{-0.607510\,\hat{r}_Q^{\cdot} - 0.635054\,\hat{g}_Q^{\cdot} + 1}, \\ g_Q^{\cdot} &= \frac{-0.003951\,\hat{r}_Q^{\cdot} + 0.575889\,\hat{g}_Q^{\cdot} + 0.009406}{-0.607510\,\hat{r}_Q^{\cdot} - 0.635054\,\hat{g}_Q^{\cdot} + 1}\ . \end{aligned} \tag{16}$$

In particular, since $(\hat{r}_{\hat{R}}^{\cdot}, \hat{g}_{\hat{R}}^{\cdot}) = (1, 0)$, $(\hat{r}_{\hat{G}}^{\cdot}, \hat{g}_{\hat{G}}^{\cdot}) = (0, 1)$, and $(\hat{r}_{\hat{B}}^{\cdot}, \hat{g}_{\hat{B}}^{\cdot}) = (0, 0)$, employing the above transformation equations shows that in the new *RGB* representation of the Stiles-Burch$_{1955}$ 2° pilot group the chromaticity coordinates of the original primaries are

$$\begin{aligned} &r_{\hat{R}}^{\cdot} = 0.987276, \quad g_{\hat{R}}^{\cdot} = 0.013898, \quad b_{\hat{R}}^{\cdot} = 1 - r_{\hat{R}}^{\cdot} - g_{\hat{R}}^{\cdot} = -0.001174, \\ &r_{\hat{G}}^{\cdot} = -0.641980, \quad g_{\hat{G}}^{\cdot} = 1.603785, \quad b_{\hat{G}}^{\cdot} = 1 - r_{\hat{G}}^{\cdot} - g_{\hat{G}}^{\cdot} = 0.038195, \\ &r_{\hat{B}}^{\cdot} = -0.016470, \quad g_{\hat{B}}^{\cdot} = 0.009406, \quad b_{\hat{B}}^{\cdot} = 1 - r_{\hat{B}}^{\cdot} - g_{\hat{B}}^{\cdot} = 1.007064\ . \end{aligned} \tag{17}$$

Figure 2 **A**: $(\hat{r}^{\cdot}, \hat{g}^{\cdot})$ chromaticity diagram of the Stiles-Burch$_{1955}$ 2° pilot group. The diagram refers to primaries $\hat{\boldsymbol{R}}^{\cdot}$, $\hat{\boldsymbol{G}}^{\cdot}$, and $\hat{\boldsymbol{B}}^{\cdot}$ representing unit radiance, monochromatic stimuli with wave numbers 15500, 19000, and 22500 cm^{-1}. Filled circles on the spectrum locus mark the chromaticity points $(R^{\cdot})$, $(G^{\cdot})$, and $(B^{\cdot})$ of the new Wright primaries. The chromaticity point (E) of Illuminant *E* is positioned at $(\hat{r}_E^{\cdot}, \hat{g}_E^{\cdot}) = (0.579468, 0.265210)$. **B**: $(r^{\cdot}, g^{\cdot})$ chromaticity diagram of the Stiles-Burch$_{1955}$ 2° pilot group resulting from transformation $T_{\hat{r}}^{r^{\cdot}}$ [Eqs. (16)]. The diagram refers to Wright primaries $\boldsymbol{R}^{\cdot}$, $\boldsymbol{G}^{\cdot}$, and $\boldsymbol{B}^{\cdot}$ representing monochromatic stimuli of wavelengths 700.0, 546.1, and 435.8 nm, normalized so that the chromaticity point (*E*) of Illuminant *E* is positioned at $(r_E^{\cdot}, g_E^{\cdot}) = (\tfrac{1}{3}, \tfrac{1}{3})$. Filled squares on the spectrum locus mark the chromaticity points $(\hat{R}^{\cdot})$, $(\hat{G}^{\cdot})$, and $(\hat{B}^{\cdot})$ of the original Stiles-Burch primaries (joined by dashed lines).

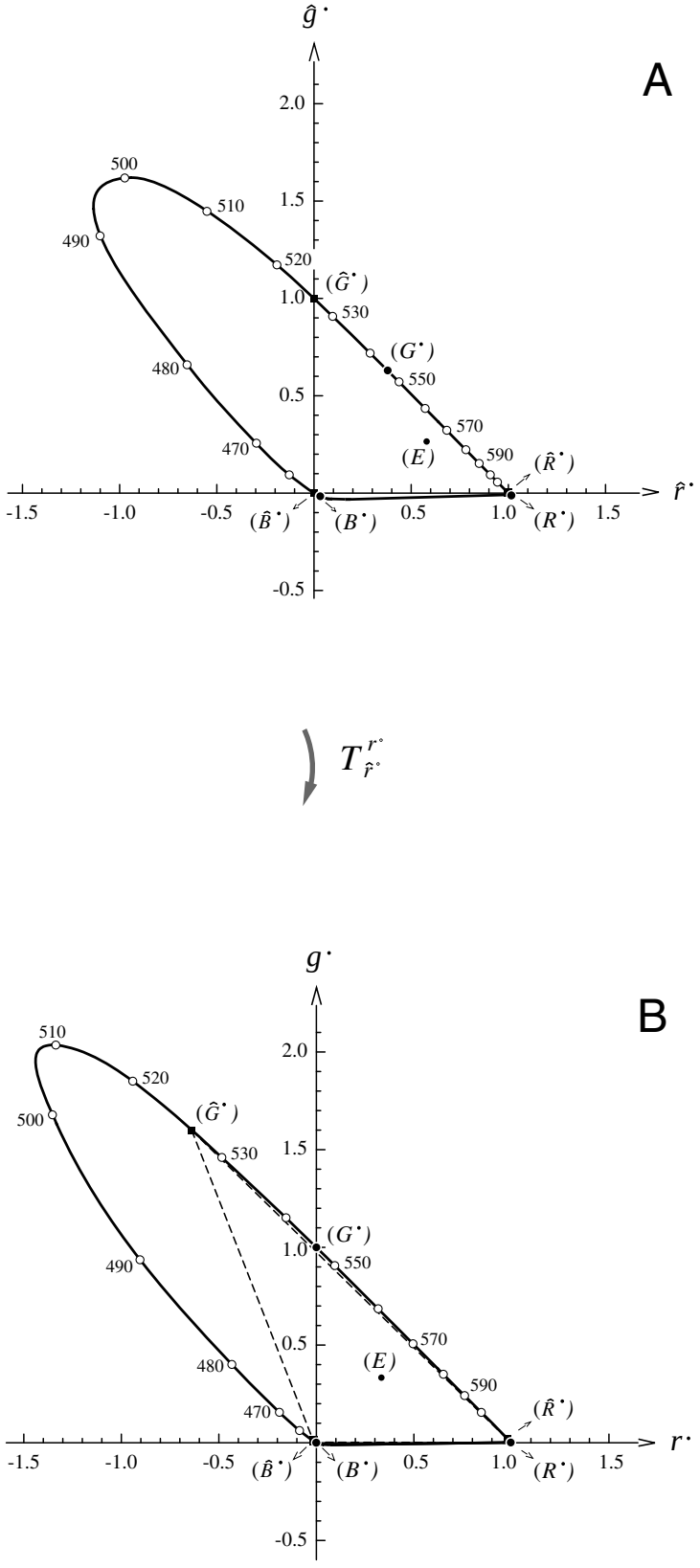
A
$\hat{g}^{\cdot}$
$\hat{r}^{\cdot}$
2.0
1.5
1.0
0.5
-0.5
-1.5
-1.0
-0.5
0.5
1.0
1.5
500
510
520
530
550
570
590
490
480
470
$(\hat{G}^{\cdot})$
$(G^{\cdot})$
(E)
$(\hat{R}^{\cdot})$
$(\hat{B}^{\cdot})$
$(B^{\cdot})$
$(R^{\cdot})$
$T^{r^{\circ}}_{\hat{r}^{\circ}}$
B
$g^{\cdot}$
$r^{\cdot}$
2.0
1.5
1.0
0.5
-0.5
-1.5
-1.0
-0.5
0.5
1.0
1.5
510
520
500
530
550
570
590
490
480
470
$(\hat{G}^{\cdot})$
$(G^{\cdot})$
(E)
$(\hat{R}^{\cdot})$
$(\hat{B}^{\cdot})$
$(B^{\cdot})$
$(R^{\cdot})$

Figure 2

Figure 2A shows the original $(\hat{r}^{\cdot}, \hat{g}^{\cdot})$ chromaticity diagram of the Stiles-Burch$_{1955}$ 2° pilot group, and Fig. 2B shows the $(r^{\cdot}, g^{\cdot})$ diagram resulting from transformation equations (16). In both diagrams are shown (1) the chromaticity points $(\hat{R}^{\cdot})$, $(\hat{G}^{\cdot})$, and $(\hat{B}^{\cdot})$ of the original primaries $\hat{\boldsymbol{R}}^{\cdot}$, $\hat{\boldsymbol{G}}^{\cdot}$, and $\hat{\boldsymbol{B}}^{\cdot}$, (2) the chromaticity points $(R^{\cdot})$, $(G^{\cdot})$, and $(B^{\cdot})$ of the new primaries $\boldsymbol{R}^{\cdot}$, $\boldsymbol{G}^{\cdot}$, and $\boldsymbol{B}^{\cdot}$ and (3) the chromaticity point (E) of Illuminant *E*.

6. CIRCUMSCRIPTION OF THE SPECTRUM LOCUS IN THE $(r^{\cdot}, g^{\cdot})$ DIAGRAM

According to the concept of the $\boldsymbol{X}^{\cdot}\boldsymbol{Y}^{\cdot}\boldsymbol{Z}^{\cdot}$ tristimulus space, in the corresponding $(r^{\cdot}, g^{\cdot})$ diagram the triangle with vertices at the chromaticity points of the primaries $\boldsymbol{X}^{\cdot}$, $\boldsymbol{Y}^{\cdot}$, and $\boldsymbol{Z}^{\cdot}$ must fully circumscribe the spectrum locus. The lines making up the triangle are denoted as follows:

- line connecting the chromaticity points of the primaries $\boldsymbol{Y}^{\cdot}$ and $\boldsymbol{Z}^{\cdot}$ (*YZ* line): $L_1^{\cdot}$;
- line connecting the chromaticity points of the primaries $\boldsymbol{X}^{\cdot}$ and $\boldsymbol{Z}^{\cdot}$ (*XZ* line): $L_2^{\cdot}$;
- line connecting the chromaticity points of the primaries $\boldsymbol{X}^{\cdot}$ and $\boldsymbol{Y}^{\cdot}$ (*XY* line): $L_3^{\cdot}$.

6.1. *XZ* Line, $L_2^{\cdot}$ (The Alychne Line)

The *XZ* line $L_2^{\cdot}$ connecting the chromaticity points of the primaries $\boldsymbol{X}^{\cdot}$ and $\boldsymbol{Z}^{\cdot}$ was taken as the line representing the alychne as defined by the synthesized spectral luminous efficiency function $V^{\cdot}(\lambda)$. As already mentioned, this function equals a linear combination of the 2° L and M fundamentals of Stockman *et al*.[30] Thus, if $L^{\cdot}(\lambda)$ and $M^{\cdot}(\lambda)$ denote these fundamentals we have

$$V^{\cdot}(\lambda) = c_L\, L^{\cdot}(\lambda) + c_M\, M^{\cdot}(\lambda)\,. \tag{18}$$

The functions $L^{\cdot}(\lambda)$ and $M^{\cdot}(\lambda)$ are given as linear combinations of the CMF's of the Stiles-Burch$_{1955}$ 2° pilot group; that is,

$$L^{\cdot}(\lambda) = \sum_{i=1}^{3} a_{Li}\, \bar{r}_i^{\cdot}(\lambda)\ , \qquad M^{\cdot}(\lambda) = \sum_{i=1}^{3} a_{Mi}\, \bar{r}_i^{\cdot}(\lambda)\,. \tag{19}$$

If we substitute $L^{\cdot}(\lambda)$ and $M^{\cdot}(\lambda)$ in Eq. (18), the equation for $V^{\cdot}(\lambda)$ takes the form

$$V^{\cdot}(\lambda) = \sum_{i=1}^{3} (c_L\, a_{Li} + c_M\, a_{Mi})\, \bar{r}_i^{\cdot}(\lambda)\,. \tag{20}$$

Since, by definition, the luminosities (as defined relative to $V^{\cdot}(\lambda)$) of the stimuli represented on the alychne (referring to $V^{\cdot}(\lambda)$) are all zero, Eq. (20) implies that the line in the original $(\hat{r}^{\cdot}, \hat{g}^{\cdot})$ diagram representing this alychne (the alychne line) is given by the equation

$$\sum_{i=1}^{3} (c_L a_{Li} + c_M a_{Mi}) \hat{r}_i^{\cdot} = 0 \ . \tag{21}$$

Substituting $\hat{r}_i^{\cdot}$ $(i = 1, 2, 3)$ using the inverse of Eqs. (10) — i.e., the transformation

$$T_{r^{\cdot}}^{\hat{r}^{\cdot}}: \quad \hat{r}_i^{\cdot} = \frac{\sum_{j=1}^{3} \mathbb{R}_{ji}^{\hat{R}^{\cdot}} r_j^{\cdot}}{\sum_{l,j=1}^{3} \mathbb{R}_{jl}^{\hat{R}^{\cdot}} r_j^{\cdot}} \ , \qquad \mathbb{R}_{ji}^{\hat{R}^{\cdot}} \equiv \frac{\hat{r}_{iE}^{\cdot} \, \mathbb{I}^{\rho \hat{R}^{\cdot}}_{ji}}{\sum_{\rho=1}^{3} \mathbb{I}^{\rho \hat{R}^{\cdot}}_{\rho i} \, r_{\rho E}^{\cdot}} \qquad (i = 1, 2, 3) \ , \tag{22}$$

with the coefficient $\mathbb{I}^{\rho \hat{R}^{\cdot}}_{ji}$ being the cofactor of element $r_{ji}^{\cdot}$ in the matrix $\left(r_{ji}^{\cdot}\right) \equiv \left(r_{j\hat{R}_i^{\cdot}}^{\cdot}\right)$ — the equation of the alychne line $L_2^{\cdot}$ in the new $(r^{\cdot}, g^{\cdot})$ diagram is determined. (Since the above transformation is a mapping of a line, indices *Q* are dropped in the transformation variables.) The equation reads

$$\sum_{i,j=1}^{3} (c_L a_{Li} + c_M a_{Mi}) \ \mathbb{R}_{ji}^{\hat{R}^{\cdot}} \ r_j^{\cdot} \ = \ 0 \, , \qquad \mathbb{R}_{ji}^{\hat{R}^{\cdot}} \equiv \frac{\hat{r}_{iE}^{\cdot} \, \mathbb{I}^{\rho \hat{R}^{\cdot}}_{ji}}{\sum_{\rho=1}^{3} \mathbb{I}^{\rho \hat{R}^{\cdot}}_{\rho i} \, r_{\rho E}^{\cdot}} \ . \tag{23}$$

According to the paper of Stockman *et al.*[30], the values of the coefficients a_{Li} $(i = 1, 2, 3)$ and a_{Mi} $(i = 1, 2, 3)$ are

$$\begin{aligned} &a_{L1} = 0.214808 \, , \quad a_{L2} = 0.751035 \, , \quad a_{L3} = 0.045156 \, , \\ &a_{M1} = 0.022882 \, , \quad a_{M2} = 0.940534 \, , \quad a_{M3} = 0.076827 \, . \end{aligned} \tag{24}$$

To further comply with the work of Stockman *et al.*[30], we decided to adopt their proposals for the values of the coefficients c_L and c_M also, i.e., [34]

$$c_L = 0.682882 \, , \qquad c_M = 0.352429 \ . \tag{25}$$

When first inserting the above values [Eqs. (24) and (25)] and the values of the chromaticity coordinates $\hat{r}_{iE}^{\cdot}$ $(i = 1, 2, 3)$ and $r_{jE}^{\cdot}$ $(j = 1, 2, 3)$ [Eqs. (14) and (15)] into Eqs. (23), then determining of the cofactors $\mathbb{I}^{\rho \hat{R}^{\cdot}}_{ji}$ $(i, j = 1, 2, 3)$ by means of the

matrix elements $r_{ji}^{\cdot}$ $(i, j = 1, 2, 3)$ [Eqs. (17)], and ultimately eliminating the coordinate $r_3^{\cdot} \equiv b^{\cdot}$ using the relation $b^{\cdot} = 1 - r^{\cdot} - g^{\cdot}$, the equation of the line $L_2^{\cdot}$ in the $(r^{\cdot}, g^{\cdot})$ diagram representing the alychne turns out to be

$$L_2^{\cdot}: \quad g^{\cdot} = \alpha_2^{\cdot}\, r^{\cdot} + \beta_2^{\cdot}\,, \quad \alpha_2^{\cdot} = -0.212634\,, \quad \beta_2^{\cdot} = -0.031615\,. \tag{26}$$

The line is shown in Fig. 3A.

6.2. *XY* line, $L_3^{\cdot}$

In conformity with the CIE concept, the *XY* line was drawn tangential to the spectrum locus in the long-wavelength region. As the first step, a set of interpolation functions for the spectral chromaticity coordinates in the *RGB* representation were determined following the procedure outlined in Appendix D. Then, with a continuous parametric representation of the spectrum locus in the $(r^{\cdot}, g^{\cdot})$ diagram at hand, a line of slope $\alpha_3^{\cdot}$ equal to the slope of the corresponding line in the Judd-Vos (r', g') diagram, i.e.,

$$\alpha_3^{\cdot} = \alpha_3' = -1.010269\,, \tag{27}$$

was made tangent to the spectrum locus at one single point $(T^{\cdot})$. The resulting *XY* line, $L_3^{\cdot}$, is shown in Fig. 3A. The inset to the right shows a magnification of the long-wavelength region of the spectrum locus. Here the ordinate $d_3^{\cdot}$ is the Euclidean distance between the points on the locus segment and their respective closest points on $L_3^{\cdot}$. The blowup shows that compared with the *XY* lines in the analogous Judd-Vos (r', g') and CIE$_{1931}$ (r, g) diagrams, the line $L_3^{\cdot}$ is shifted slightly to the right. This parallel shift is due to a small convexity in the long-wavelength region of the spectrum locus in the $(r^{\cdot}, g^{\cdot})$ diagram, a convexity not present in the other two diagrams. An alternative procedure would have been to smooth the color matching data of the red flank of the spectrum before drawing the tangent line. However, not knowing whether the convexity reflects some significant physiological mechanism, such as rod intruision[35] or other influences, we decided to keep the data unchanged.

By means of numerical calculations, the tangent point $(T^{\cdot})$ between the *XY* line $L_3^{\cdot}$ and the spectrum locus is determined to be $(r_{T^{\cdot}}^{\cdot}, g_{T^{\cdot}}^{\cdot}) = (0.979429,\ 0.021946)$, which corresponds to the parameter value $\lambda_{T^{\cdot}} = 637.849$ nm. Combined with the value of $\alpha_3^{\cdot}$, this implies that the equation of the chosen *XY* line is

$$L_3^{\cdot}: \quad g^{\cdot} = \alpha_3^{\cdot}\, r^{\cdot} + \beta_3^{\cdot}\,, \quad \alpha_3^{\cdot} = -1.010269\,, \quad \beta_3^{\cdot} = 1.011432\,. \tag{28}$$

The point $(P^{\cdot})$ of intersection between $L_3^{\cdot}$ and the abscissa axis turns out to be $(r_{P\cdot}^{\cdot}, g_{P\cdot}^{\cdot}) = (1.001152,\ 0)$. In comparison, the corresponding points in the Judd-Vos (r', g') and CIE $_{1931}$ (r, g) diagrams are $(r'_{P'}, g'_{P'}) = (1.000029,\ 0)$ and $(r_P, g_P) = (1, 0)$, respectively.

6.3. *YZ* line, $L_1^{\cdot}$

As already mentioned, the criteria imposed on the *YZ* line are the following:

– The distance $d_{1D\cdot}^{\cdot}$ from the closest point $(D^{\cdot})$ on the spectrum locus (the locus being interpolated as outlined in Appendix D) is to equal the corresponding distance in the Judd-Vos (r', g') diagram; that is,

$$d_{1D\cdot}^{\cdot} = d'_{1D'} = 0.020365. \tag{29}$$

– The slope of the line is to be adjusted so that the vertices of the resulting circumscribing triangle define the chromaticity points of new primaries $\boldsymbol{X}^{\cdot}$, $\boldsymbol{Y}^{\cdot}$, and $\boldsymbol{Z}^{\cdot}$ providing the basis for an $(x^{\cdot}, y^{\cdot})$ diagram whose spectrum locus differs as little as possible from the spectrum locus in the Judd-Vos (x', y') diagram.

To be specific, the latter criterion requires that the Euclidean difference between the two spectrum loci be minimum according to a least-RMS criterion, calculated at 1-nm intervals.

If we assume that none of the lines $L_1^{\cdot}$, $L_2^{\cdot}$, and $L_3^{\cdot}$ in the $(r^{\cdot}, g^{\cdot})$ diagram are parallel to the ordinate axis, it follows from Eqs. (C.2) and (C.4) of Appendix C that, by once again using Illuminant *E* as a normalization stimulus, the transformation $T_{r\cdot}^{x\cdot}$ from the chromaticity coordinates $r_Q^{\cdot}$ and $g_Q^{\cdot}$ to the new chromaticity coordinates $x_{kQ}^{\cdot}$ $(k = 1, 2, 3)$ can be expressed by the equations

$$x_{kQ}^{\cdot} = \frac{x_{kE}^{\cdot}\,\dfrac{\alpha_k^{\cdot} r_Q^{\cdot} - g_Q^{\cdot} + \beta_k^{\cdot}}{\alpha_k^{\cdot} r_E^{\cdot} - g_E^{\cdot} + \beta_k^{\cdot}}}{\displaystyle\sum_{m=1}^{3} x_{mE}^{\cdot}\,\frac{\alpha_m^{\cdot} r_Q^{\cdot} - g_Q^{\cdot} + \beta_m^{\cdot}}{\alpha_m^{\cdot} r_E^{\cdot} - g_E^{\cdot} + \beta_m^{\cdot}}} \qquad (k = 1, 2, 3)\ . \tag{30}$$

The coefficient $\alpha_k^{\cdot}$ is here the slope of $L_k^{\cdot}$ and the coefficient $\beta_k^{\cdot}$ the ordinate at the point of intersection between $L_k^{\cdot}$ and the ordinate axis. In the case of monochromatic stimuli, the index *Q* is replaced by λ, and the resulting symbols $x_{k\lambda}^{\cdot}$ $(k = 1, 2, 3)$, $r_{\lambda}^{\cdot}$

and $g_\lambda^{\cdot}$ then denote the chromaticity coordinates of a monochromatic stimulus of the wavelength specified.

Regarding the slope of the *YZ* line, this can be expressed as a function of the wavelength parameter $\lambda_{D\cdot}$ at the locus point $(D^{\cdot})$ of shortest distance to the line. The function is [36]

$$\alpha_1^{\cdot}(\lambda_{D\cdot}) = \frac{\left.\frac{d}{d\lambda}[g^{\cdot}(\lambda)]\right|_{\lambda=\lambda_{D\cdot}}}{\left.\frac{d}{d\lambda}[r^{\cdot}(\lambda)]\right|_{\lambda=\lambda_{D\cdot}}} \quad . \tag{31}$$

Here $r^{\cdot}(\lambda)$ and $g^{\cdot}(\lambda)$ are the spectral chromaticity coordinate functions derived as outlined in Appendix D. Given the shortest distance $d_{1D\cdot}^{\cdot}$ from the *YZ* line to the spectrum locus, it then follows that the ordinate at the point of intersection between this line and the ordinate axis is expressed as a function of $\lambda_{D\cdot}$ by the equation

$$\beta_1^{\cdot}(\lambda_{D\cdot}) = g_\lambda^{\cdot}(\lambda_{D\cdot}) - \alpha_1^{\cdot}(\lambda_{D\cdot})\, r_\lambda^{\cdot}(\lambda_{D\cdot}) - d_{1D\cdot}^{\cdot}\sqrt{\alpha_1^{\cdot}(\lambda_{D\cdot})^2 + 1} \; . \tag{32}$$

When calculated for every nanometer, the RMS of the Euclidean difference between the spectrum locus of the new $(x^{\cdot}, y^{\cdot})$ diagram and that of the Judd-Vos (x', y') diagram (the reference diagram) is interpreted as

$$\text{RMS} = \sqrt{\frac{1}{341}\sum_{\lambda=390}^{730}\sum_{k=1}^{2}(x_{k\lambda}^{\cdot} - x_{k\lambda}')^2} \; , \tag{33}$$

with $341 = 730 - 390 + 1$ being the number of tabulated values in the 1-nm tabulations of the Stiles-Burch$_{1955}$ 2° pilot group[31]. Thus, the least RMS criterion outlined above is fulfilled when the wavelength parameter $\lambda_{D\cdot}$ at the locus point $(D^{\cdot})$ of shortest distance to the *YZ* line minimizes the function

$$\Delta(\lambda_{D\cdot}) = \sum_{\lambda=390}^{730}\sum_{k=1}^{2}\left(\frac{x_{kE}^{\cdot}\,\dfrac{\alpha_k^{\cdot} r_\lambda^{\cdot} - g_\lambda^{\cdot} + \beta_k^{\cdot}}{\alpha_k^{\cdot} r_E^{\cdot} - g_E^{\cdot} + \beta_k^{\cdot}}}{\displaystyle\sum_{m=1}^{3} x_{mE}^{\cdot}\,\frac{\alpha_m^{\cdot} r_\lambda^{\cdot} - g_\lambda^{\cdot} + \beta_m^{\cdot}}{\alpha_m^{\cdot} r_E^{\cdot} - g_E^{\cdot} + \beta_m^{\cdot}}} - x_{k\lambda}'\right)^2 \Bigg|_{\substack{\alpha_1^{\cdot} = \alpha_1^{\cdot}(\lambda_{D\cdot}) \\ \beta_1^{\cdot} = \beta_1^{\cdot}(\lambda_{D\cdot})}} . \tag{34}$$

After

(1) ensuring normalization of the new *XYZ* representation according to CIE's criterion by assigning to the coordinates $x_{kE}^{\cdot}$ $(k = 1, 2, 3)$ the values

$$x_{1E}^{\cdot} \equiv x_E^{\cdot} = \tfrac{1}{3}, \qquad x_{2E}^{\cdot} \equiv y_E^{\cdot} = \tfrac{1}{3}, \qquad x_{3E}^{\cdot} \equiv z_E^{\cdot} = \tfrac{1}{3}; \tag{35}$$

(2) inserting the values of $r_E^{\cdot}$, $g_E^{\cdot}$, $\alpha_k^{\cdot}$ $(k = 2, 3)$, $\beta_k^{\cdot}$ $(k = 2, 3)$, and $d_{1D}^{\cdot}$. [Eqs. (15), (26), (28), and (29)];

(3) computing interpolated values for the coordinates $x'_{k\lambda}$ ($\lambda = 390$ nm, 391 nm, ..., 730 nm) $(k = 1, 2)$ in the way outlined in Appendix D;

(4) using the Eqs. (16) (with index *Q* replaced by λ) to determine the coordinates $r_\lambda^{\cdot}$ and $g_\lambda^{\cdot}$ ($\lambda = 390$ nm, 391 nm, ..., 730 nm) from the 1-nm tabulations of the Stiles-Burch$_{1955}$ 2° pilot group [31];

numerical minimization shows that $\Delta(\lambda_{D^{\cdot}})$ is minimum at $\lambda_{D^{\cdot},\,min} = 501.662$ nm, implying that $(D^{\cdot})$ is given as $(r_{D^{\cdot}}^{\cdot}, g_{D^{\cdot}}^{\cdot}) = (-1.398789, 1.788181)$. The corresponding least-RMS value is $\mathrm{RMS}_{min} = 0.021411$.

If $\alpha_1^{\cdot}$ denotes the slope of the optimized *YZ* line $L_1^{\cdot}$, and $\beta_1^{\cdot}$ denotes the ordinate of its intersection with the ordinate axis, the two are given as $\alpha_1^{\cdot} = \alpha_1^{\cdot}(\lambda_{D^{\cdot},\,min})$ and $\beta_1^{\cdot} = \beta_1^{\cdot}(\lambda_{D^{\cdot},\,min})$. Thus, calculating the function values, $L_1^{\cdot}$ is shown to be given by the equation

$$L_1^{\cdot}: \quad g^{\cdot} = \alpha_1^{\cdot}\, r^{\cdot} + \beta_1^{\cdot}, \quad \alpha_1^{\cdot} = -2.629242, \quad \beta_1^{\cdot} = -1.946861. \tag{36}$$

The line is shown in Fig. 3A. In the inset to the left, showing a magnification of the spectrum locus in the vicinity of $(D^{\cdot})$, the ordinate $d_1^{\cdot}$ is the Euclidean distance between the points on the locus segment and their respective closest points on $L_1^{\cdot}$.

6.4. Optimized Circumscribing Triangle

Given that the lines $L_k^{\cdot}$ $(k = 1, 2, 3)$ constituting the optimized circumscribing triangle are known, the coordinates of its vertices — i.e. the chromaticity coordinates $r_{1k}^{\cdot} \equiv r_{X_k}^{\cdot}$ and $r_{2k}^{\cdot} \equiv g_{X_k}^{\cdot}$ of the new primaries $\boldsymbol{X}_k^{\cdot}$ $(k = 1, 2, 3)$ — are given by the equations

$$r_{1k}^{\cdot} = \frac{\beta_j^{\cdot} - \beta_i^{\cdot}}{\alpha_i^{\cdot} - \alpha_j^{\cdot}}, \quad r_{2k}^{\cdot} = \frac{\alpha_i^{\cdot}\,\beta_j^{\cdot} - \alpha_j^{\cdot}\,\beta_i^{\cdot}}{\alpha_i^{\cdot} - \alpha_j^{\cdot}} \qquad (i, j, k = 1,2,3 \text{ and } i \neq j \neq k \neq i). \tag{37}$$

On insertion of the values given in Eqs. (26), (28), and (36) the coordinates turn out to be

$$r_{11}^{\cdot} \equiv r_{X^{\cdot}}^{\cdot} = 1.307675, \quad r_{21}^{\cdot} \equiv g_{X^{\cdot}}^{\cdot} = -0.309671, \quad r_{31}^{\cdot} \equiv b_{X^{\cdot}}^{\cdot} = 1 - r_{X^{\cdot}}^{\cdot} - g_{X^{\cdot}}^{\cdot} = 0.001996,$$

$$r_{12}^{\cdot} \equiv r_{Y^{\cdot}}^{\cdot} = -1.827264, \quad r_{22}^{\cdot} \equiv g_{Y^{\cdot}}^{\cdot} = 2.857460, \quad r_{32}^{\cdot} \equiv b_{Y^{\cdot}}^{\cdot} = 1 - r_{Y^{\cdot}}^{\cdot} - g_{Y^{\cdot}}^{\cdot} = -0.030196, \quad (38)$$

$$r_{13}^{\cdot} \equiv r_{Z^{\cdot}}^{\cdot} = -0.792535, \quad r_{23}^{\cdot} \equiv g_{Z^{\cdot}}^{\cdot} = 0.136905, \quad r_{33}^{\cdot} \equiv b_{Z^{\cdot}}^{\cdot} = 1 - r_{Z^{\cdot}}^{\cdot} - g_{Z^{\cdot}}^{\cdot} = 1.655630 \ .$$

Since the vertices of the circumscribing triangle define the chromaticity points of the new primaries, they are labeled $(X^{\cdot})$, $(Y^{\cdot})$, and $(Z^{\cdot})$ in Fig. 3A.

7. $(x^{\cdot}, y^{\cdot})$ CHROMATICITY DIAGRAM OF THE STILES-BURCH$_{1955}$ 2° PILOT GROUP

With the circumscribing triangle thus established, the derivation of the new $(x^{\cdot}, y^{\cdot})$ diagram is now straightforward. According to Eq. (A3) of Appendix A, the transformation from chromaticity coordinates $r_{jQ}^{\cdot}$ $(j = 1, 2, 3)$ to chromaticity coordinates $x_{kQ}^{\cdot}$ $(k = 1, 2, 3)$ is

$$T_{r^{\cdot}}^{x^{\cdot}} : \quad x_{kQ}^{\cdot} = \frac{\sum_{j=1}^{3} \mathbb{R}_{jk}^{X^{\cdot}} r_{jQ}^{\cdot}}{\sum_{m,j=1}^{3} \mathbb{R}_{jm}^{X^{\cdot}} r_{jQ}^{\cdot}} \ , \qquad \mathbb{R}_{jk}^{X^{\cdot}} \equiv \frac{x_{kE}^{\cdot} \, \mathbb{I}^{\circ}{}_{jk}^{X^{\cdot}}}{\sum_{\mu=1}^{3} \mathbb{I}^{\circ}{}_{\mu k}^{X^{\cdot}} r_{\mu E}^{\cdot}} \qquad (k = 1, 2, 3) \ , \qquad (39)$$

with $\mathbb{I}^{\circ}{}_{jk}^{X^{\cdot}}$ being the cofactor of element $r_{jk}^{\cdot}$ in the matrix $r_{jk}^{\cdot} \equiv \left(r_{jX_k^{\cdot}}^{\cdot} \right)$. When first determining the cofactors $\mathbb{I}^{\circ}{}_{jk}^{X^{\cdot}}$ $(j, k = 1, 2, 3)$ by means of the matrix elements $r_{jk}^{\cdot}$ $(j, k = 1, 2, 3)$ [Eqs. (38)], then inserting the values of the chromaticity coordinates $r_{jE}^{\cdot}$ $(j = 1, 2, 3)$ and $x_{kE}^{\cdot}$ $(k = 1, 2, 3)$ [Eqs. (15) and (35)], and ultimately eliminating the

---

Figure 3 **A**: $(r^{\cdot}, g^{\cdot})$ chromaticity diagram of the Stiles-Burch$_{1955}$ 2° pilot group (same as the diagram of Figure 2B) with lines $L_1^{\cdot}$, $L_2^{\cdot}$, and $L_3^{\cdot}$ (dashed) constituting a circumscribing triangle with vertices corresponding to the chromaticity points $(X^{\cdot})$, $(Y^{\cdot})$, and $(Z^{\cdot})$ of the new primaries $\boldsymbol{X}^{\cdot}$, $\boldsymbol{Y}^{\cdot}$, and $\boldsymbol{Z}^{\cdot}$. Ordinates $d_1^{\cdot}$ and $d_3^{\cdot}$ of the inset magnifications give the Euclidean distances between the points on the locus segments (framed) and their respective closest points on the lines $L_1^{\cdot}$ and $L_3^{\cdot}$. Point $(D^{\cdot})$ marks the locus point of shortest distance to line $L_1^{\cdot}$. Line $L_3^{\cdot}$ is tangent to the spectrum locus at point $(T^{\cdot})$ and intersects the abscissa axis in $(P^{\cdot})$. **B**: $(x^{\cdot}, y^{\cdot})$ chromaticity diagram of the Stiles-Burch$_{1955}$ 2° pilot group resulting from transformation $T_{r^{\cdot}}^{x^{\cdot}}$ [Eqs. (40)]. Filled circles on the spectrum locus mark the chromaticity points $(R^{\cdot})$, $(G^{\cdot})$, and $(B^{\cdot})$ of the Wright primaries underlying the $(r^{\cdot}, g^{\cdot})$ diagram. The chromaticity point (E) of Illuminant E is positioned at $(x_E^{\cdot}, y_E^{\cdot}) = (\frac{1}{3}, \frac{1}{3})$.

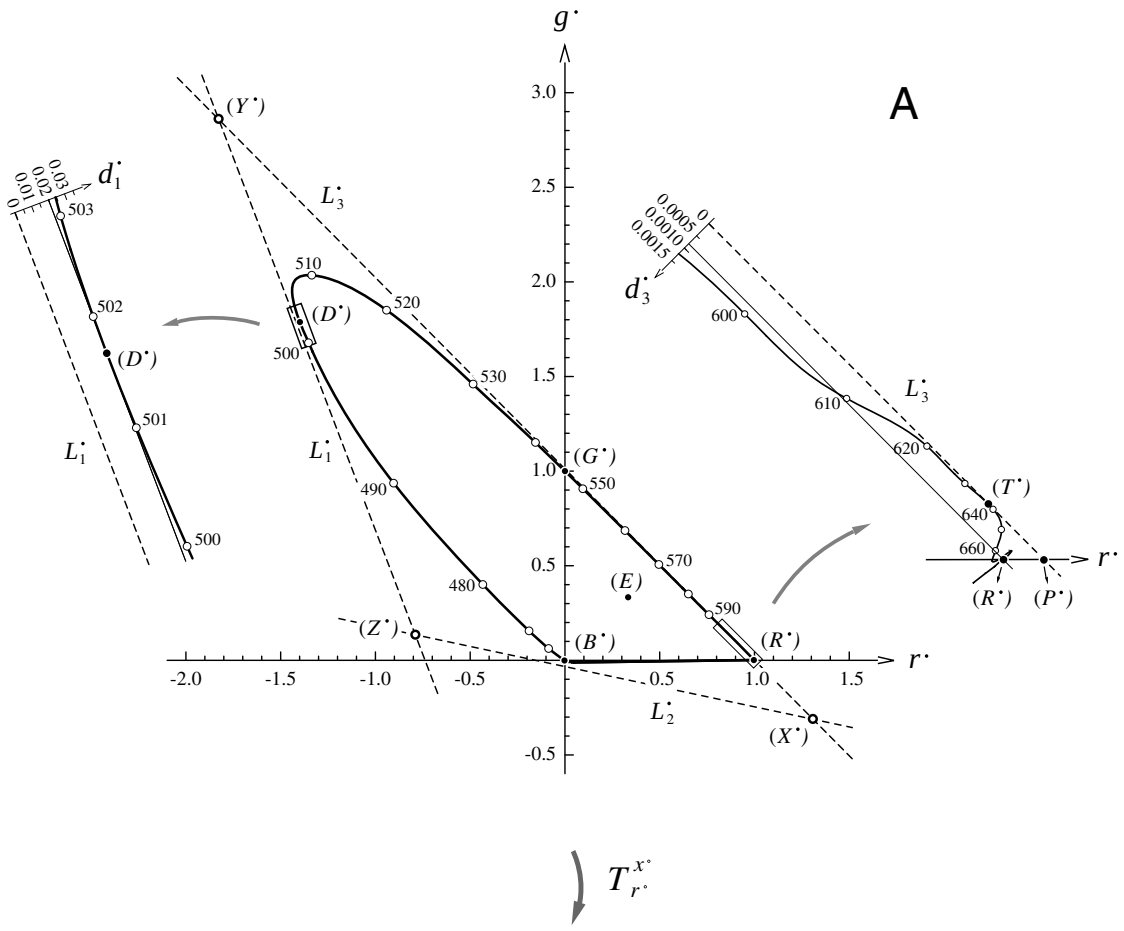

$T_{r^{\cdot}}^{x^{\cdot}}$

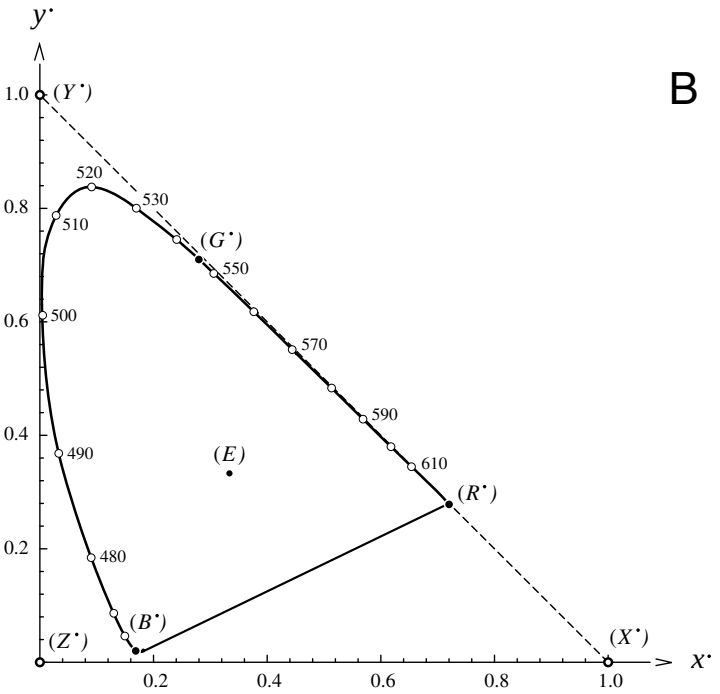

Figure 3

coordinate $r_{3Q}^{\cdot} \equiv b_Q^{\cdot}$ using the relation $b_Q^{\cdot} = 1 - r_Q^{\cdot} - g_Q^{\cdot}$, the equations transforming the chromaticity coordinates $r_Q^{\cdot}$ and $g_Q^{\cdot}$ into new coordinates $x_Q^{\cdot}$ and $y_Q^{\cdot}$ turn out to be[37]

$$x_Q^{\cdot} = \frac{0.228051\, r_Q^{\cdot} + 0.086736\, g_Q^{\cdot} + 0.168864}{-0.448711\, r_Q^{\cdot} - 0.087153\, g_Q^{\cdot} + 1},$$

$$y_Q^{\cdot} = \frac{0.133580\, r_Q^{\cdot} + 0.628216\, g_Q^{\cdot} + 0.019861}{-0.448711\, r_Q^{\cdot} - 0.087153\, g_Q^{\cdot} + 1}\ . \tag{40}$$

In particular, since $(r_{R\cdot}^{\cdot}, g_{R\cdot}^{\cdot}) = (1, 0)$, $(r_{G\cdot}^{\cdot}, g_{G\cdot}^{\cdot}) = (0, 1)$, and $(r_{B\cdot}^{\cdot}, g_{B\cdot}^{\cdot}) = (0, 0)$, employing the above transformation equations shows that in the final *XYZ* representation of the Stiles-Burch$_{1955}$ 2° pilot group, the chromaticity coordinates of the Wright primaries $\boldsymbol{R}^{\cdot}$, $\boldsymbol{G}^{\cdot}$, and $\boldsymbol{B}^{\cdot}$ are:

$$\begin{aligned}
&x_{R\cdot}^{\cdot} = 0.719976, \quad y_{R\cdot}^{\cdot} = 0.278331, \quad z_{R\cdot}^{\cdot} = 1 - x_{R\cdot}^{\cdot} - y_{R\cdot}^{\cdot} = 0.001693,\\
&x_{G\cdot}^{\cdot} = 0.280003, \quad y_{G\cdot}^{\cdot} = 0.709951, \quad z_{G\cdot}^{\cdot} = 1 - x_{G\cdot}^{\cdot} - y_{G\cdot}^{\cdot} = 0.010046,\\
&x_{B\cdot}^{\cdot} = 0.168864, \quad y_{B\cdot}^{\cdot} = 0.019861, \quad z_{B\cdot}^{\cdot} = 1 - x_{B\cdot}^{\cdot} - y_{B\cdot}^{\cdot} = 0.811275\ .
\end{aligned} \tag{41}$$

The concept of the circumscription of the spectrum locus in the $(r^{\cdot}, g^{\cdot})$ diagram is sketched in Figure 3A, and the $(x^{\cdot}, y^{\cdot})$ diagram resulting from the transformation Eqs. (40) is shown in Figure 3B. Plotted in both diagrams are (1) the chromaticity points $(R^{\cdot})$, $(G^{\cdot})$, and $(B^{\cdot})$ of the Wright primaries $\boldsymbol{R}^{\cdot}$, $\boldsymbol{G}^{\cdot}$, and $\boldsymbol{B}^{\cdot}$; (2) the chromaticity points $(X^{\cdot})$, $(Y^{\cdot})$, and $(Z^{\cdot})$ of the new primaries $\boldsymbol{X}^{\cdot}$, $\boldsymbol{Y}^{\cdot}$, and $\boldsymbol{Z}^{\cdot}$ and (3) the chromaticity point (E) of Illuminant *E*.

8. COMPOSITE TRANSFORMATION EQUATIONS

Now that the new $(x^{\cdot}, y^{\cdot})$ diagram has been created with the help of an intermediate $(r^{\cdot}, g^{\cdot})$ diagram, what remains is to determine the direct-route transformation from chromaticity coordinates $\hat{r}_{iQ}^{\cdot}$ $(i = 1, 2, 3)$ in the Stiles-Burch original $\hat{R}\hat{G}\hat{B}$ representation into chromaticity coordinates $x_{kQ}^{\cdot}$ $(k = 1, 2, 3)$ in the new *XYZ* representation. According to Eqs. (B.11) of Appendix B, this composite transformation, $T_{\hat{r}\cdot}^{x\cdot} \equiv T_{\hat{r}\cdot}^{r\cdot} \circ T_{r\cdot}^{x\cdot}$, is given as

$$T_{\hat{r}\cdot}^{x\cdot} \equiv T_{\hat{r}\cdot}^{r\cdot} \circ T_{r\cdot}^{x\cdot}: \quad x_{kQ}^{\cdot} = \frac{\sum_{i=1}^{3} \hat{\mathbb{R}}_{ik}^{X\cdot}\, \hat{r}_{iQ}^{\cdot}}{\sum_{n,i=1}^{3} \hat{\mathbb{R}}_{in}^{X\cdot}\, \hat{r}_{iQ}^{\cdot}}, \quad \hat{\mathbb{R}}_{ik}^{X\cdot} \equiv \sum_{j=1}^{3} \frac{(r_{jE}^{\cdot}\, x_{kE}^{\cdot})\,(\hat{\mathbb{r}}_{ij}^{R\cdot}\, \mathbb{r}_{jk}^{X\cdot})}{\sum_{\rho,\mu=1}^{3} (\hat{\mathbb{r}}_{\rho j}^{R\cdot}\, \mathbb{r}_{\mu k}^{X\cdot})\,(\hat{r}_{\rho E}^{\cdot}\, r_{\mu E}^{\cdot})} \quad (k = 1,2,3). \tag{42}$$

When first determining the values of the cofactors $\hat{\mathcal{I}}^{R\cdot}_{ij}$ $(i, j = 1, 2, 3)$ and $\mathcal{I}^{X\cdot}_{jk}$ $(j, k = 1, 2, 3)$ (see previous sections), then inserting the values of the chromaticity coordinates of Illuminant *E* in the three representations in question [Eqs. (14), (15), and (35)], and ultimately eliminating the coordinate $x_{3Q}^{\cdot} \equiv z_Q^{\cdot}$ using the relation $z_Q^{\cdot} = 1 - x_Q^{\cdot} - y_Q^{\cdot}$, the final equations transforming the chromaticity coordinates $\hat{r}_Q^{\cdot}$ and $\hat{g}_Q^{\cdot}$ into the new coordinates $x_Q^{\cdot}$ and $y_Q^{\cdot}$ turn out to be:

$$x_Q^{\cdot} = \frac{-0.010734\,\hat{r}_Q^{\cdot} - 0.106262\,\hat{g}_Q^{\cdot} + 0.164841}{-0.783283\,\hat{r}_Q^{\cdot} - 0.583672\,\hat{g}_Q^{\cdot} + 1},$$

$$y_Q^{\cdot} = \frac{0.039157\,\hat{r}_Q^{\cdot} + 0.317985\,\hat{g}_Q^{\cdot} + 0.023416}{-0.783283\,\hat{r}_Q^{\cdot} - 0.583672\,\hat{g}_Q^{\cdot} + 1}. \qquad (43)$$

For completeness, we also calculate the inverse equations. These are

$$\hat{r}_Q^{\cdot} = \frac{443.553255\,x_Q^{\cdot} + 13.440336\,y_Q^{\cdot} - 73.430328}{302.544303\,x_Q^{\cdot} + 102.938188\,y_Q^{\cdot} + 1},$$

$$\hat{g}_Q^{\cdot} = \frac{-76.898538\,x_Q^{\cdot} + 158.326203\,y_Q^{\cdot} + 8.968607}{302.544303\,x_Q^{\cdot} + 102.938188\,y_Q^{\cdot} + 1}. \qquad (44)$$

Since $(\hat{r}_{\hat{R}}^{\cdot}, \hat{g}_{\hat{R}}^{\cdot}) = (1, 0)$, $(\hat{r}_{\hat{G}}^{\cdot}, \hat{g}_{\hat{G}}^{\cdot}) = (0, 1)$, and $(\hat{r}_{\hat{B}}^{\cdot}, \hat{g}_{\hat{B}}^{\cdot}) = (0, 0)$, employing the transformation Eqs. (43) shows that in the new *XYZ* representation of the Stiles-Burch$_{1955}$ 2° pilot group, the chromaticity coordinates of the original primaries $\hat{\boldsymbol{R}}^{\cdot}$, $\hat{\boldsymbol{G}}^{\cdot}$, and $\hat{\boldsymbol{B}}^{\cdot}$ are

$$\begin{aligned}
&x_{\hat{R}}^{\cdot} = 0.711098, \quad y_{\hat{R}}^{\cdot} = 0.288731, \quad z_{\hat{R}}^{\cdot} = 1 - x_{\hat{R}}^{\cdot} - y_{\hat{R}}^{\cdot} = 0.000171,\\
&x_{\hat{G}}^{\cdot} = 0.140704, \quad y_{\hat{G}}^{\cdot} = 0.820029, \quad z_{\hat{G}}^{\cdot} = 1 - x_{\hat{G}}^{\cdot} - y_{\hat{G}}^{\cdot} = 0.039267, \qquad (45)\\
&x_{\hat{B}}^{\cdot} = 0.164841, \quad y_{\hat{B}}^{\cdot} = 0.023416, \quad z_{\hat{B}}^{\cdot} = 1 - x_{\hat{B}}^{\cdot} - y_{\hat{B}}^{\cdot} = 0.811743\ .
\end{aligned}$$

Likewise, given that $(x_X^{\cdot}, y_X^{\cdot}) = (1, 0)$, $(x_Y^{\cdot}, y_Y^{\cdot}) = (0, 1)$, $(x_Z^{\cdot}, y_Z^{\cdot}) = (0, 0)$, the chromaticity coordinates of the new primaries $\boldsymbol{X}^{\cdot}$, $\boldsymbol{Y}^{\cdot}$, and $\boldsymbol{Z}^{\cdot}$ in Stiles and Burch's original $\hat{R}\hat{G}\hat{B}$ representation are determined to be

$$\hat{r}_{X\cdot}^{\cdot} = 1.219337\,, \qquad \hat{g}_{X\cdot}^{\cdot} = -0.223789\,, \qquad \hat{b}_{X\cdot}^{\cdot} = 0.004452\,,$$
$$\hat{r}_{Y\cdot}^{\cdot} = -0.577170\,, \qquad \hat{g}_{Y\cdot}^{\cdot} = 1.609561\,, \qquad \hat{b}_{Y\cdot}^{\cdot} = -0.032391\,, \qquad (46)$$
$$\hat{r}_{Z\cdot}^{\cdot} = -73.430328\,, \qquad \hat{g}_{Z\cdot}^{\cdot} = 8.968607\,, \qquad \hat{b}_{Z\cdot}^{\cdot} = 65.461721\,.$$

Because of the rather remote location of the chromaticity point $(\hat{r}_{Z\cdot}^{\cdot}\,,\, \hat{g}_{Z\cdot}^{\cdot})$ of the primary $\boldsymbol{Z}^{\cdot}$, a figure showing the circumscription of the spectrum locus in the original $(\hat{r}^{\cdot}\,,\, \hat{g}^{\cdot})$ diagram has not been included.

At this point, the only task left for a complete description of the new *XYZ* representation of the Stiles-Burch $_{1955}$ 2° pilot group is the derivation of the linear transformation $T_{\bar{r}\cdot}^{\bar{X}\cdot}$ that transform the CMF's of the original $\hat{R}\hat{G}\hat{B}$ representation into a set of CMF's referring to the new primaries $\boldsymbol{X}^{\cdot}$, $\boldsymbol{Y}^{\cdot}$, and $\boldsymbol{Z}^{\cdot}$. According to Eqs. (B.10) of Appendix B, $T_{\bar{r}\cdot}^{\bar{X}\cdot}$ is expressed in the form of a composite transformation as follows:

$$T_{\bar{r}\cdot}^{\bar{X}\cdot} \equiv T_{\bar{r}\cdot}^{\bar{r}\cdot} \circ T_{\bar{r}\cdot}^{\bar{X}\cdot}: \qquad \bar{x}_k^{\cdot}(\lambda) = \kappa \sum_{i=1}^{3} \hat{\mathbb{R}}_{ik}^{X\cdot}\, \bar{\hat{r}}_i^{\cdot}(\lambda)\,,$$
$$\hat{\mathbb{R}}_{ik}^{X\cdot} \equiv \sum_{j=1}^{3} \frac{(r_{jE}^{\cdot}\, x_{kE}^{\cdot})\,(\hat{\mathbb{r}}_{ij}^{R\cdot}\; \mathbb{r}_{jk}^{X\cdot})}{\sum_{\rho,\mu=1}^{3} (\hat{\mathbb{r}}_{\rho j}^{R\cdot}\; \mathbb{r}_{\mu k}^{X\cdot})\,(\hat{r}_{\rho E}^{\cdot}\, r_{\mu E}^{\cdot})}\,, \qquad \kappa \neq 0 \qquad (k = 1,\, 2,\, 3). \qquad (47)$$

To determine the common factor κ, an additional criterion is required, and in order to comply with the existing CIE standard the criterion imposed is $\bar{y}^{\cdot}(\lambda) \equiv \bar{x}_2^{\cdot}(\lambda) \equiv V^{\cdot}(\lambda)$. Together with Eq. (20) the above equation with index $k = 2$ then gives

$$\sum_{i=1}^{3} (c_L\, a_{Li} + c_M\, a_{Mi})\, \bar{\hat{r}}_i^{\cdot}(\lambda) = \kappa \sum_{i=1}^{3} \hat{\mathbb{R}}_{i2}^{X\cdot}\, \bar{\hat{r}}_i^{\cdot}(\lambda)\,, \qquad (48)$$

from which it follows that

$$\kappa = \frac{c_L\, a_{Li} + c_M\, a_{Mi}}{\hat{\mathbb{R}}_{i2}^{X\cdot}} \qquad i \in \{1,\, 2,\, 3\} \qquad (49)$$

(since the CMF's $\bar{\hat{r}}_i^{\cdot}(\lambda)$ $(k = 1,\, 2,\, 3)$ are linearly independent).

Substituting κ in transformation Eqs. (47) and subsequently inserting the values of the relevant cofactors (the same as in Eqs. (10) and (40)), coefficients [Eqs. (24) and (25)] and chromaticity coordinates of Illuminant *E* [Eqs. (14), (15) and (35)], the matrix equation that transforms the CMF's $\bar{\hat{r}}^{\cdot}(\lambda) \equiv \bar{\hat{r}}_1^{\cdot}(\lambda)$, $\bar{\hat{g}}^{\cdot}(\lambda) \equiv \bar{\hat{r}}_2^{\cdot}(\lambda)$, and $\bar{\hat{b}}^{\cdot}(\lambda) \equiv \bar{\hat{r}}_3^{\cdot}(\lambda)$ in

Stiles-Burch's original $\hat{R}\hat{G}\hat{B}$ representation into CMF's $\bar{x}^{\cdot}(\lambda) \equiv \bar{x}_1^{\cdot}(\lambda)$, $\bar{y}^{\cdot}(\lambda) \equiv \bar{x}_2^{\cdot}(\lambda)$, and $\bar{z}^{\cdot}(\lambda) \equiv \bar{x}_3^{\cdot}(\lambda)$ defining the Stiles-Burch$_{1955}$ $\boldsymbol{X}^{\cdot}\boldsymbol{Y}^{\cdot}\boldsymbol{Z}^{\cdot}$ tristimulus space turns out to be

$$\begin{pmatrix} \bar{x}^{\cdot}(\lambda) \\ \bar{y}^{\cdot}(\lambda) \\ \bar{z}^{\cdot}(\lambda) \end{pmatrix} = \begin{pmatrix} 0.381130 & 0.144873 & 0.407677 \\ 0.154753 & 0.844339 & 0.057912 \\ 0.000091 & 0.040433 & 2.007571 \end{pmatrix} \begin{pmatrix} \bar{\hat{r}}^{\cdot}(\lambda) \\ \bar{\hat{g}}^{\cdot}(\lambda) \\ \bar{\hat{b}}^{\cdot}(\lambda) \end{pmatrix} . \qquad (50)$$

The CMF's resulting from this transformation are plotted in Fig. 4A. For comparison, the CMF's $\bar{x}'(\lambda)$, $\bar{y}'(\lambda)$, and $\bar{z}'(\lambda)$ that define the Judd-Vos $\boldsymbol{X}'\boldsymbol{Y}'\boldsymbol{Z}'$ tristimulus space (the reference system) are shown in Fig. 4B.

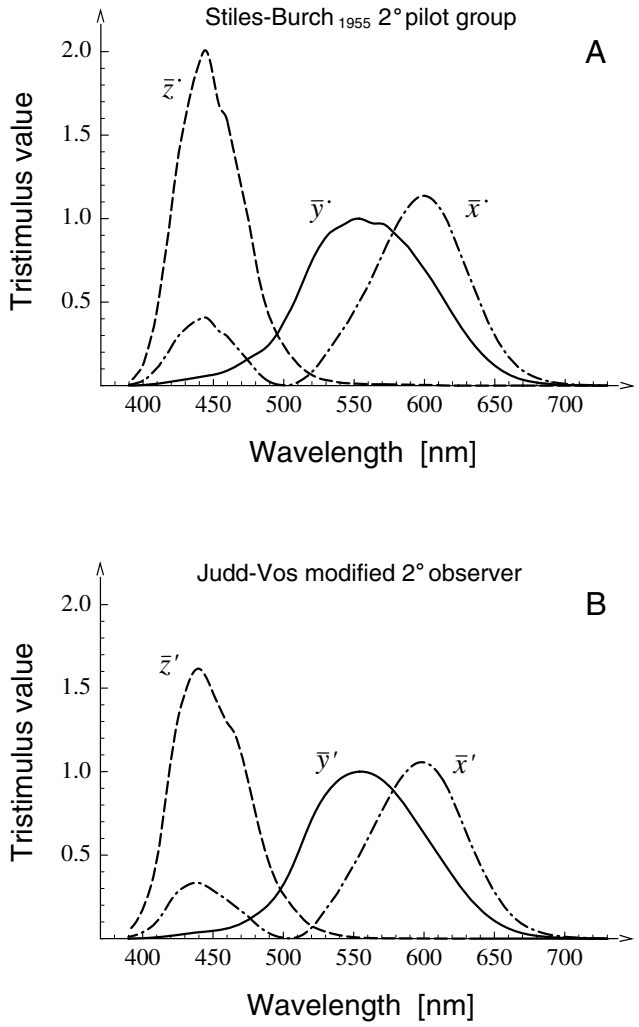

Figure 4 **A**: Color-matching functions defining the new Stiles-Burch$_{1955}$ $\boldsymbol{X}^{\cdot}\boldsymbol{Y}^{\cdot}\boldsymbol{Z}^{\cdot}$ tristimulus space. **B**: Color-matching functions defining the Judd-Vos $\boldsymbol{X}'\boldsymbol{Y}'\boldsymbol{Z}'$ tristimulus space.

9. DISCUSSION

Due to certain shortcomings of the CIE_{1931} standard colorimetric system[3,4,32], the CIE technical committee TC 1-36 has been engaged in developing a new physiologically based colorimetric system.[1] Although this new system in principle need not be accompanied by an *XYZ* representation, it will certainly be advantageous to prepare for comparison with the old standard by bringing forth a representation similar to the well established *XYZ* systems.[9]

With this in mind, the present work describes a general and precise method for the derivation of *XYZ* representations. Since, in developing the CIE_{1931} *XYZ* system, some of the criteria were rather loosely formulated, the main goal here has been to make explicit a set of criteria which (1) applies to any set of color matching data and (2) unequivocally define an *XYZ* representation. To avoid ambiguity, some additional criteria had to be implemented. We have chosen to relate these criteria to the geometrical properties of a triangle circumscribing the spectrum locus in the chromaticity diagram of an intermediate *RGB* representation (based on Wright primaries representing monochromatic stimuli of wavelengths 700.0, 546.5, and 435.8 nm). In particular, one of the criteria imposed by us is that the spectrum locus in the chromaticity diagram of the new *XYZ* representation is to deviate as little as possible from the spectrum locus in the (x', y') diagram of the Judd-Vos modified 2° observer[19,20]. This database has been invaluable to color scientists for several decades.

To illustrate our method, we have on the preceding pages derived a $\text{Stiles-Burch}_{1955}$ $\boldsymbol{X}^{\cdot}\boldsymbol{Y}^{\cdot}\boldsymbol{Z}^{\cdot}$ tristimulus space and a corresponding $(x^{\cdot}, y^{\cdot})$ diagram. The difference between the latter and the (x', y') diagram of Judd-Vos is illustrated in Fig. 5 where the spectrum loci are displayed in a joint coordinate system having double-labeled axes. In the inset diagram, the Euclidean distances $s_\lambda \equiv \sqrt{(x_\lambda^{\cdot} - x_\lambda')^2 + (y_\lambda^{\cdot} - y_\lambda')^2}$ between pairs of corresponding points are displayed as a function of the wavelength parameter λ. As seen from the inset, the most pronounced discrepancies between the two diagrams are found for parameter values between approximately 470 and 515 nm. The main plot shows that in this region the displacement vectors are directed roughly along the spectrum loci. Since the chromaticity point of Illuminant *E* is nearly the same in the two diagrams, the displacement vectors will become shorter as purity decreases toward the white point.

The above discrepancies have their origin predominantly in real differences between the color matches determined by the two groups of observers. This is apparent

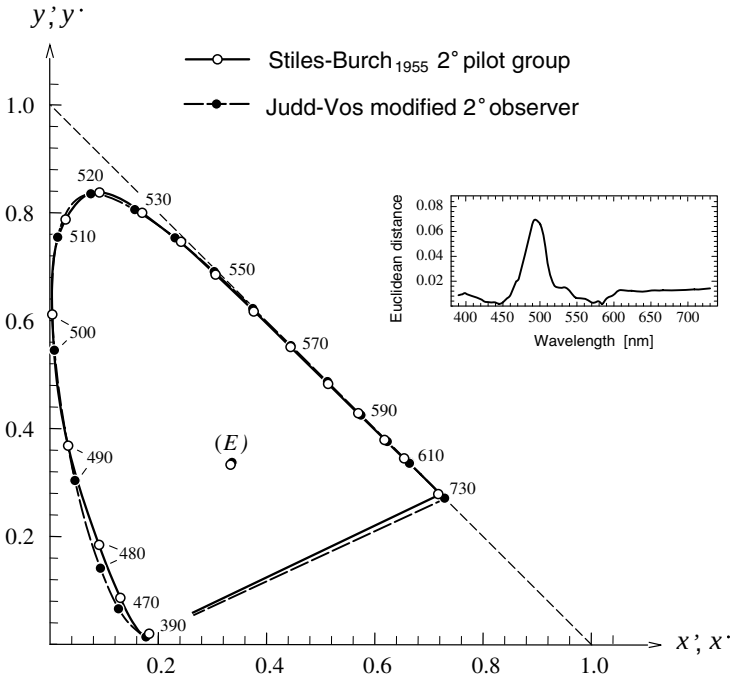

Figure 5 Joint plot displaying the spectrum locus of the new Stiles-Burch $(x^{\cdot}, y^{\cdot})$ diagram (solid curve) together with the spectrum locus of the Judd-Vos (x', y') diagram used as reference (dashed curve). The corresponding two coordinate points of Illuminant *E* are shown to be slightly separated. In the inset diagram the Euclidean distances $s_\lambda \equiv \sqrt{(x_\lambda^{\cdot} - x_\lambda')^2 + (y_\lambda^{\cdot} - y_\lambda')^2}$ between corresponding points on the spectrum loci are displayed as a function of the wavelength parameter λ.

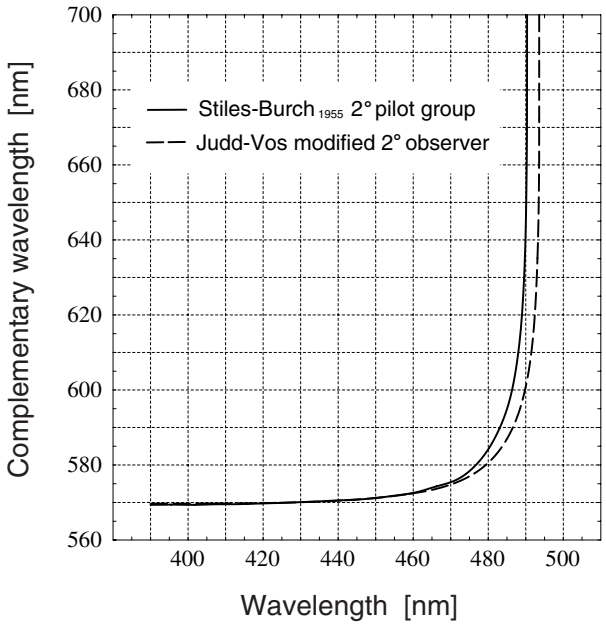

Figure 6 Complementary wavelengths of the Stiles-Burch$_{1955}$ 2° pilot group (solid curve) and the Judd-Vos modified 2° observer (dashed curve).

from a comparison of their complementary wavelengths (by necessity, reflecting characteristics of the observer groups and not of the representations). As shown in Fig. 6, for the Judd-Vos modified 2° observer the monochromatic stimuli from the long-wavelength flank of the spectrum are complementary to monochromatic stimuli of wavelengths up to between 493 and 494 nm (by calculation 493.67 nm), whereas for the Stiles-Burch$_{1955}$ 2° pilot group the corresponding wavelengths are shorter and limited upward to just above 490 nm (by calculation 490.36 nm).

With regard to the CMF's derived by our method, a comment is needed on the shape of $\bar{y}^{\cdot}(\lambda)$. As seen from the graph in Fig. 4A, $\bar{y}^{\cdot}(\lambda)$ is not as smooth as the corresponding function $\bar{y}'(\lambda)$ of Fig. 4B. In our procedure there is no way of avoiding this since, on combining the L and M fundamentals of Stockman *et al.*[30] so that the result resembles the spectral luminous efficiency function, the function $\bar{y}^{\cdot}(\lambda) \equiv V^{\cdot}(\lambda)$ is the curve obtained by adopting their proposed weighting factors [Eqs. (25)]. Even though these weighting factors may not be optimal, it nevertheless turns out that a curve that (1) fits the CIE$_{1988}$ 2° spectral luminous efficiency function[38] $V_M(\lambda) \equiv \bar{y}'(\lambda)$ satisfactorily and (2) is totally free of irregularities cannot be synthesized by any linear combination of the fundamental L and M response curves.

At this point we may recall Sperling's finding that individual spectral luminous efficiency functions for 2° fields, determined by flicker photometry, tend to show bends that are quite similar to those of $\bar{y}^{\cdot}(\lambda)$.[39] It may therefore be that the irregularities of $\bar{y}^{\cdot}(\lambda) \equiv V^{\cdot}(\lambda)$, which at first glance may be interpreted as artifacts, actually reflect characteristics of the eye's luminous sensitivity that are apparent neither from the averaged spectral luminous efficiency function $V(\lambda)$ of the CIE$_{1924}$ photometric observer[19] nor from the CIE$_{1988}$ 2° spectral luminous efficiency function[38] $V_M(\lambda)$ of the Judd-Vos modified 2° observer (the two functions being identical for $\lambda \geq 460$). Taking into account the mixed origin of the 1924 $V(\lambda)$, this may not be unlikely.

Regarding the more general aspects of our presentation, purely geometrical considerations motivated the requirement that in the chromaticity diagram of the intermediate *RGB* representation the line connecting the chromaticity points of the *X* and *Y* primaries be tangent to the spectrum locus while having the same slope as the corresponding line in a chosen reference diagram. An alternative and somewhat stricter criterion, which takes physiological considerations into account, is to require that the CMF's that refers to the new *Z* primary be equal to the fundamental S response curve (S fundamental). In the chromaticity diagram of the *RGB*

representation, the *XY* line is then fixed by this criterion alone. Moreover, since the *XZ* line is already determined by the luminous efficiency function adopted, the chromaticity point of the *X*-primary — i.e., the point of intersection between the *XY* and the *XZ* line — is fixed as well. Hence what remains will be to optimize the *YZ* line by using the criterion of minimal deviation from the chosen reference diagram. The advantage of introducing this alternative criterion is that only the *X* primary has no physiological correlate. (The CMF that refers to the *Y* primary will resemble the spectral luminous efficiency function, traceable to magnocellular units in the visual pathway. The CMF that refers to the *Z* primary will equal the S fundamental, which derives from S cones.) However, a condition that must be fulfilled for success with this approach is that the S fundamental can be expressed as a linear combination of the CMF's used as a database. Unfortunately, the 2° fundamental S response curve, $S^{\cdot}(\lambda)$, of Stockman *et al.*[30] cannot, like their proposed L and M fundamentals ($L^{\cdot}(\lambda)$ and $M^{\cdot}(\lambda)$), be expressed as a linear combination of the CMF's of the Stiles-Burch$_{1955}$ 2° pilot group. The S fundamental equals such a combination only in the wavelength region up to 525 nm. As a consequence of this lack of linear relationship, protanopic and deuteranopic confusion points corresponding to the fundamentals of Stockman *et al.* [30] are not properly defined in a chromaticity diagram referring to the Stiles-Burch$_{1955}$ 2° pilot group. Only the tritanopic confusion point $(S^{\cdot})$ can be determined precisely. For wavelengths longer than 525 nm, however, the values of both the S fundamental $S^{\cdot}(\lambda)$ and the function $S^{\cdot}_{lin}(\lambda)$ obtained by extending the range of the linear relationship to include the entire visible spectrum are quite small. Therefore the chromaticity points $(L^{\cdot}_{lin})$ and $(M^{\cdot}_{lin})$, representing the primaries that the L and M fundamentals of Stockman *et al.* would be referring to if their S fundamental been replaced by $S^{\cdot}_{lin}(\lambda)$, can be taken as reasonable estimates of the protanopic and had deuteranopic confusion points. The positions of $(L^{\cdot}_{lin})$ and $(M^{\cdot}_{lin})$ in the new $(x^{\cdot}, y^{\cdot})$ diagram are determined to be $(x^{\cdot}_{L^{\cdot}_{lin}}, y^{\cdot}_{L^{\cdot}_{lin}}) = (0.737988, 0.262181)$ and $(x^{\cdot}_{M^{\cdot}_{lin}}, y^{\cdot}_{M^{\cdot}_{lin}}) = (1.350806, -0.342893)$. The tritanopic confusion point $(S^{\cdot})$, which in contrast to $(L^{\cdot}_{lin})$ and $(M^{\cdot}_{lin})$ is strictly consistent with the fundamentals of Stockman *et al.*, is located at $(x^{\cdot}_{S^{\cdot}}, y^{\cdot}_{S^{\cdot}}) = (0.175618, 0)$. The loci of $(L^{\cdot}_{lin})$, $(M^{\cdot}_{lin})$, and $(S^{\cdot})$ in the $(x^{\cdot}, y^{\cdot})$ diagram are shown in Fig. 7. The solid lines marked $L^{\cdot} = 0$ and $M^{\cdot} = 0$ and the dashed line marked $S^{\cdot}_{lin} = 0$ represent the (virtual) stimuli for which, respectively, the fundamental L , M and (approximate) S response — i.e., the tristimulus value referring respectively to the L , M and (slightly modified) S fundamental of Stockman *et al.* — is zero.

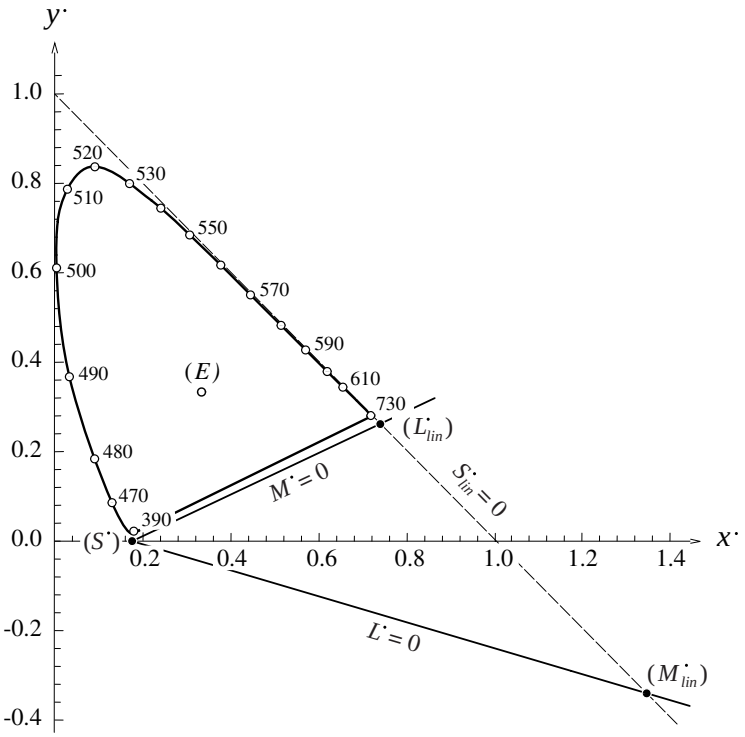

Figure 7 The $(x^{\cdot}, y^{\cdot})$ chromaticity diagram of the Stiles-Burch$_{1955}$ 2° pilot group showing (estimated) locations of the dichromatic confusion points (filled circles). Point $(S^{\cdot})$ is the tritanopic confusion point as determined relative to the original cone fundamentals of Stockman *et al.*[30] Points $(L^{\cdot}_{lin})$ and $(M^{\cdot}_{lin})$ represent the primaries that the L and M fundamentals of Stockman *et al.* would be referring to if the domain of their S fundamental's linear relationship to the CMF's of the Stiles-Burch$_{1955}$ 2° pilot group were extended to include the entire visible spectrum. The lines marked $L^{\cdot} = 0$ and $M^{\cdot} = 0$ (solid) and the line marked $S^{\cdot}_{lin} = 0$ (dashed) represent the (virtual) stimuli for which respectively the fundamental L , M and (approximate) S response is zero.

The drawback of imposing a criterion that ties up still another CMF (the one referring to the *Z* primary) is that with this stricter constraint the correspondence between the derived chromaticity diagram and the one used as reference will be worsened. Therefore whether to impose this criterion becomes a question of evaluating the benefits of improved physiological relevance relative to the deterioration of conformity.

An alternative method based on minimization of the difference between the CMF's of the new *XYZ* representation and those of the chosen reference system is discussed in Refs. 21 and 22 (see also Ref. 20).

ACKNOWLEDGMENTS

We would like to thank Inger Rudvin, Thorstein Seim, Hans Vos, and David Brainard for valuable comments and Françoise Viénot and Peter Walraven for their encouragement during this work.

APPENDICES

Appendix A: General Transformations (Formulation 1)

There exists an infinite number of colorimetrically equivalent representations of tristimulus space, but often particular tasks may require specific representations. In such cases, the adequate representations of the CMF's and the associated chromaticity coordinates are obtained by means of linear and projective transformations, respectively.

Let

- $\boldsymbol{V}_j$ ($j = 1, 2, 3$) denote the primaries of the new representation (the new
- primaries);
- $\bar{u}_i(\lambda)$ ($i = 1, 2, 3$) denote the CMF's in the old representation;
- $\bar{v}_j(\lambda)$ ($j = 1, 2, 3$) denote the CMF's in the new representation;
- u_{iQ} ($i = 1, 2, 3$) denote the chromaticity coordinates of a stimulus Q in the old representation;
- v_{jQ} ($j = 1, 2, 3$) denote the chromaticity coordinates of a stimulus Q in the new representation;
- u_{ij} ($i, j = 1, 2, 3$) denote the chromaticity coordinates of the new primaries $\boldsymbol{V}_j$ ($j = 1, 2, 3$) in the old representation — i.e. $u_{ij} \equiv u_{iV_j}$ ($i, j = 1, 2, 3$) ;
- U_{ij}^{V} denote the cofactor of element u_{ij} in the matrix $\left(u_{ij}\right) \equiv \left(u_{iV_j}\right)$ — i.e. the matrix whose j^{th} column consists of the chromaticity coordinates of the new primary $\boldsymbol{V}_j$ in the old representation.

If N is a stimulus whose chromaticity coordinates in the new representation satisfy $v_{jN} \neq 0$ ($j = 1, 2, 3$) (see Figs. 8A-B), the transformations in question are given as follows:

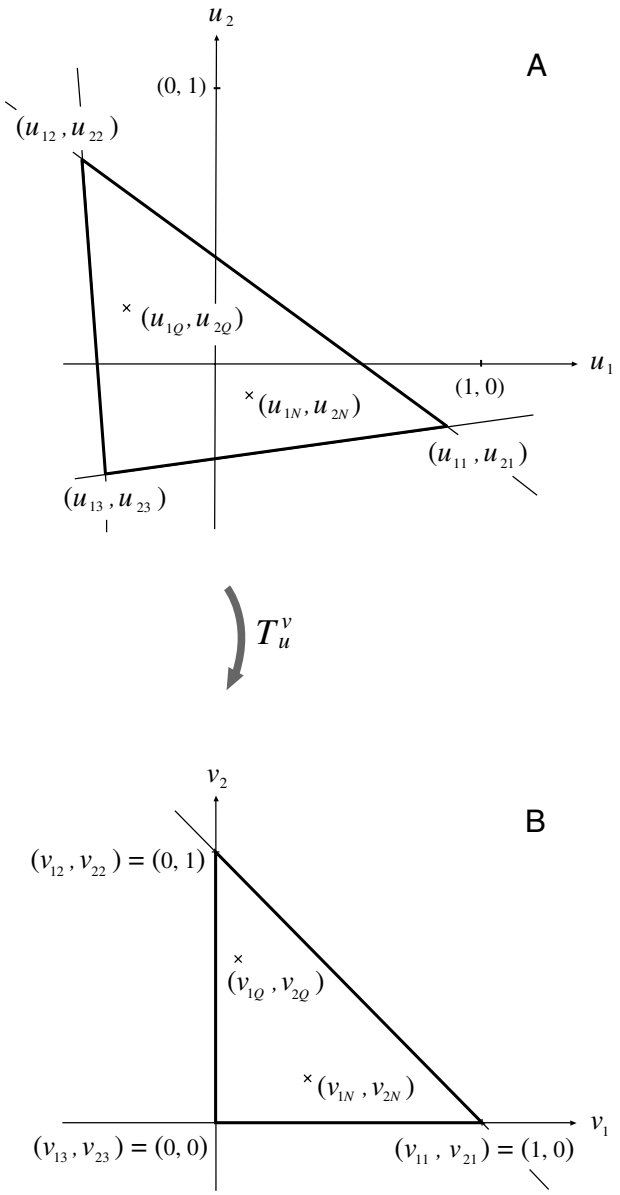

Figure 8 **A**: (u_1,u_2) chromaticity diagram referring to primaries $\boldsymbol{U}_i$ (i = 1,2,3). The vertices of the solid triangle define the chromaticity points of the primaries $\boldsymbol{V}_j$ (j = 1,2,3) chosen as basis for the new representation. The normalization stimulus *N* must not be represented on any of the lines connecting the chromaticity points of the new primaries, but apart from this restriction it can be chosen freely. (In particular, *N* does not necessarily have to be real.) **B**: (v_1,v_2) chromaticity diagram resulting from transformation T_u^v. Because of the restrictions imposed on the choice of normalization stimulus, *N* will not be represented on any of the lines connecting the points (1, 0), (0, 1), and (0, 0), i.e. the chromaticity points of the underlying primaries $\boldsymbol{V}_j$ (j = 1,2,3).

Transformation of color-matching functions (linear):

$$T_{\bar{u}}^{\bar{v}}: \quad \bar{v}_j(\lambda) = \kappa \sum_{i=1}^{3} \mathbb{U}_{ij}^{V}\, \bar{u}_i(\lambda)\ , \quad \mathbb{U}_{ij}^{V} \equiv \frac{v_{jN}\, \mathbb{u}_{ij}^{V}}{\sum_{\rho=1}^{3} \mathbb{u}_{\rho j}^{V}\, u_{\rho N}}\ , \qquad \text{(A.1)}$$

$$\kappa \neq 0 \qquad (j = 1, 2, 3)$$

Transformation of chromaticity coordinates (projective):

$$T_{u}^{v}: \quad v_{jQ} = \frac{\sum_{i=1}^{3} \mathbb{U}_{ij}^{V}\, u_{iQ}}{\sum_{l,i=1}^{3} \mathbb{U}_{il}^{V}\, u_{iQ}}\ , \qquad \mathbb{U}_{ij}^{V} \equiv \frac{v_{jN}\, \mathbb{u}_{ij}^{V}}{\sum_{\rho=1}^{3} \mathbb{u}_{\rho j}^{V}\, u_{\rho N}} \qquad \text{(A.2)}$$

$$(j = 1, 2, 3)$$

The mutual scaling of the CMF's is determined exclusively by the chromaticity coordinates of *N* in the two representations. The absolute scaling is achieved by also determining the common factor κ. Often this factor is given by a certain criterion imposed on the sum of the three CMF's or simply on one of the functions alone. (For instance, in transforming the *RGB* representation of the CIE_{1931} 2° observer into the standard *XYZ* representation, κ is given by the criterion $\bar{y}(\lambda) \equiv V(\lambda)$.)

The coefficients $\mathbb{U}_{ij}^{V}$ $(i, j = 1, 2, 3)$ are (by a common factor) proportional to the cofactors of the corresponding elements U_{ij} of the matrix $\left(U_{ij}\right) \equiv \left(U_{iV_j}\right)$ — i.e., the matrix whose j^{th} column consists of the tristimulus values U_{iV_j} $(i = 1, 2, 3)$ of the new primary $\boldsymbol{V}_j$ in the old representation.

The reason for requiring that the chromaticity coordinates of stimulus *N* (the normalization stimulus) are to satisfy $v_{jN} \neq 0$ $(j = 1, 2, 3)$ is that the transformation is to be unequivocally defined. With regard to the chromaticity coordinates in the old representation, this same requirement implies that $\sum_{\rho=1}^{3} \mathbb{u}_{\rho j}^{V}\, u_{\rho N} \neq 0$ $(j = 1, 2, 3)$. In principle, the chromaticity of *N* can be chosen freely within this restriction. (In particular, *N* does not necessarily have to be a real stimulus.) However, in most cases

it will be convenient to let *N* equal one of the CIE standard illuminants (for instance Illuminant *E*) and further to make *N* constitute the basic stimulus of the new representation by choosing $v_{jN} = \frac{1}{3}$ ($j = 1, 2, 3$).

Complete derivations of the above transformations are given elsewhere.[40]

Appendix B: Composite Transformations

Given the transformations (see Appendix A)

$$T_{\bar{u}}^{\bar{v}}: \quad \bar{v}_j(\lambda) = \sigma \sum_{i=1}^{3} U_{ij}^{V} \bar{u}_i(\lambda) , \quad U_{ij}^{V} \equiv \frac{v_{jN} u_{ij}^{V}}{\sum_{\rho=1}^{3} u_{\rho j}^{V} u_{\rho N}} , \quad \sigma \neq 0 \quad (j = 1, 2, 3) ; \quad \text{(B.1)}$$

$$T_{u}^{v}: \quad v_{jQ} = \frac{\sum_{i=1}^{3} U_{ij}^{V} u_{iQ}}{\sum_{l,i=1}^{3} U_{il}^{V} u_{iQ}} , \quad U_{ij}^{V} \equiv \frac{v_{jN} u_{ij}^{V}}{\sum_{\rho=1}^{3} u_{\rho j}^{V} u_{\rho N}} \qquad (j = 1, 2, 3) , \qquad \text{(B.2)}$$

and

$$T_{\bar{v}}^{\bar{w}}: \quad \bar{w}_k(\lambda) = \tau \sum_{j=1}^{3} V_{jk}^{W} \bar{v}_j(\lambda) , \quad V_{jk}^{W} \equiv \frac{w_{kN} v_{jk}^{W}}{\sum_{\mu=1}^{3} v_{\mu k}^{W} v_{\mu N}} , \quad \tau \neq 0 \quad (k = 1, 2, 3) ; \quad \text{(B.3)}$$

$$T_{v}^{w}: \quad w_{kQ} = \frac{\sum_{j=1}^{3} V_{jk}^{W} v_{jQ}}{\sum_{m,j=1}^{3} V_{jm}^{W} v_{jQ}} , \quad V_{jk}^{W} \equiv \frac{w_{kN} v_{jk}^{W}}{\sum_{\mu=1}^{3} v_{\mu k}^{W} v_{\mu N}} \qquad (k = 1, 2, 3) , \qquad \text{(B.4)}$$

the transformations from CMF's $\bar{u}_i(\lambda)$ ($i = 1, 2, 3$) to CMF's $\bar{w}_k(\lambda)$ ($k = 1, 2, 3$) and from chromaticity coordinates u_{iQ} ($i = 1, 2, 3$) to chromaticity coordinates w_{kQ} ($k = 1, 2, 3$) are derived as follows:

$$\bar{w}_k(\lambda) = \tau \sum_{j=1}^{3} V_{jk}^{W} \bar{v}_j(\lambda) = \tau \sum_{j=1}^{3} V_{jk}^{W} \left(\sigma \sum_{i=1}^{3} U_{ij}^{V} \bar{u}_i(\lambda) \right) =$$

$$= \sigma\tau \sum_{j=1}^{3} \left(\sum_{i=1}^{3} U_{ij}^{V} V_{jk}^{W} \right) \bar{u}_i(\lambda) \qquad (k = 1, 2, 3) , \qquad \text{(B.5)}$$

$$w_{kQ} = \frac{\sum_{j=1}^{3} \mathbb{V}_{jk}^{W} v_{jQ}}{\sum_{m,j=1}^{3} \mathbb{V}_{jm}^{W} v_{jQ}} = \frac{\sum_{j=1}^{3} \mathbb{V}_{jk}^{W} \left(\frac{\sum_{i=1}^{3} \mathbb{U}_{ij}^{V} u_{iQ}}{\sum_{l,i=1}^{3} \mathbb{U}_{il}^{V} u_{iQ}} \right)}{\sum_{m,j=1}^{3} \mathbb{V}_{jm}^{W} \left(\frac{\sum_{i=1}^{3} \mathbb{U}_{ij}^{V} u_{iQ}}{\sum_{l,i=1}^{3} \mathbb{U}_{il}^{V} u_{iQ}} \right)} = \frac{\sum_{i=1}^{3} \left(\sum_{j=1}^{3} \mathbb{U}_{ij}^{V} \mathbb{V}_{jk}^{W} \right) u_{iQ}}{\sum_{m,i=1}^{3} \left(\sum_{j=1}^{3} \mathbb{U}_{ij}^{V} \mathbb{V}_{jm}^{W} \right) u_{iQ}} \quad (k = 1,2,3). \quad \text{(B.6)}$$

Since, according to Eqs. (A.1) and (A.2), the general forms of the transformations are

$$T_{\bar{u}}^{\bar{w}}: \quad \bar{w}_k(\lambda) = \kappa \sum_{i=1}^{3} \mathbb{U}_{ik}^{W} \bar{u}_i(\lambda) \ , \quad \mathbb{U}_{ik}^{W} \equiv \frac{w_{kN}\, \mathbb{u}_{ik}^{W}}{\sum_{\nu=1}^{3} \mathbb{u}_{\nu k}^{W} u_{\nu N}} \ , \quad \kappa \neq 0 \quad (k = 1, 2, 3) \ ; \quad \text{(B.7)}$$

$$T_{u}^{w}: \quad w_{kQ} = \frac{\sum_{i=1}^{3} \mathbb{U}_{ik}^{W} u_{iQ}}{\sum_{n,i=1}^{3} \mathbb{U}_{in}^{W} u_{iQ}} \ , \quad \mathbb{U}_{ik}^{W} \equiv \frac{w_{kN}\, \mathbb{u}_{ik}^{W}}{\sum_{\nu=1}^{3} \mathbb{u}_{\nu k}^{V} u_{\nu N}} \quad (k = 1, 2, 3) \ , \quad \text{(B.8)}$$

it is seen that

$$\mathbb{U}_{ik}^{W} = \frac{\sigma\tau}{\kappa} \sum_{j=1}^{3} \mathbb{U}_{ij}^{V} \mathbb{V}_{jk}^{W} =$$

$$= \omega \sum_{j=1}^{3} \left(\frac{v_{jN}\, \mathbb{u}_{ij}^{V}}{\sum_{\rho=1}^{3} \mathbb{u}_{\rho j}^{V} u_{\rho N}} \right) \left(\frac{w_{kN}\, \mathbb{v}_{jk}^{W}}{\sum_{\mu=1}^{3} \mathbb{v}_{\mu k}^{W} v_{\mu N}} \right) = \omega \sum_{j=1}^{3} \frac{(v_{jN} w_{kN})(\mathbb{u}_{ij}^{V} \mathbb{v}_{jk}^{W})}{\sum_{\rho,\mu=1}^{3} (\mathbb{u}_{\rho j}^{V} \mathbb{v}_{\mu k}^{W})(u_{\rho N} v_{\mu N})} \ , \quad \omega = \frac{\sigma\tau}{\kappa} \neq 0 \ . \quad \text{(B.9)}$$

Consequently, if $T_{\bar{u}}^{\bar{w}}$ and T_{u}^{w} are the compositions $T_{\bar{u}}^{\bar{v}} \circ T_{\bar{v}}^{\bar{w}}$ and $T_{u}^{v} \circ T_{v}^{w}$, these can be expressed as follows:

$$T_{\bar{u}}^{\bar{w}} \equiv T_{\bar{u}}^{\bar{v}} \circ T_{\bar{v}}^{\bar{w}}: \ \bar{w}_k(\lambda) = \kappa \sum_{i=1}^{3} \mathbb{U}_{ik}^{W} \bar{u}_i(\lambda) \ ,$$

$$\mathbb{U}_{ik}^{W} = \sum_{j=1}^{3} \frac{(v_{jN} w_{kN})(\mathbb{u}_{ij}^{V} \mathbb{v}_{jk}^{W})}{\sum_{\rho,\mu=1}^{3} (\mathbb{u}_{\rho j}^{V} \mathbb{v}_{\mu k}^{W})(u_{\rho N} v_{\mu N})} \ , \quad \kappa \neq 0 \quad (k = 1, 2, 3) \ ; \quad \text{(B.10)}$$

$$T_u^{\,w} \equiv T_u^{\,v} \circ T_v^{\,w}: \qquad w_{kQ} = \frac{\sum_{i=1}^{3} \mathbb{U}_{ik}^{W}\, u_{iQ}}{\sum_{n,\,i=1}^{3} \mathbb{U}_{in}^{W}\, u_{iQ}}, \tag{B.11}$$

$$\mathbb{U}_{ik}^{W} = \sum_{j=1}^{3} \frac{(v_{jN}\, w_{kN})\,(\mathbb{u}_{ij}^{V}\, \mathbb{w}_{jk}^{W})}{\sum_{\rho,\,\mu=1}^{3} (\mathbb{u}_{\rho j}^{V}\, \mathbb{w}_{\mu k}^{W})\,(u_{\rho N}\, v_{\mu N})} \qquad (k = 1,\, 2,\, 3)\ .$$

For simplicity, the proportionality factor ω, originally embodied in the coefficient $\mathbb{U}_{ik}^{W}$, has been dropped here since the factor cancels out in the expression for w_{kQ}. To be precise, this implies that in the transformation expressions (B.10) and (B.11) the coefficients $\mathbb{U}_{ik}^{W}$ differ by the factor ω from their counterparts in the transformation expressions (B.7) and (B.8).

Appendix C: General Transformations (Formulation 2)

Instead of expressing the transformations $T_{\bar{u}}^{\bar{v}}$ and T_u^{v} in terms of the chromaticity coordinates of the new primaries in the old representation (see Appendix A), the transformations can be expressed in terms of the equation coefficients of the lines in the old chromaticity diagram connecting the chromaticity points of the new primaries.

Let L_k be the line that connect the chromaticity points of the new primaries $\boldsymbol{V}_i$ and $\boldsymbol{V}_j$ $(i, j, k = 1, 2, 3$ and $i \neq j \neq k \neq i)$. Provided that

(1) L_k is not parallel to the ordinate axis, let

- α_k $(k = 1, 2, 3)$ denote the slope of L_k
- β_k $(k = 1, 2, 3)$ denote the ordinate at the point of intersection between L_k and the ordinate axis,

(2) L_k is not parallel to the abscissa axis, let

- α_k^* $(k = 1, 2, 3)$ denote the inverse of the slope of L_k
- β_k^* $(k = 1, 2, 3)$ denote the abscissa at the point of intersection between L_k and the abscissa axis.

Furthermore, for any finite numbers $K_k > 0$ $(k = 1, 2, 3)$ define

$$\bar{\boldsymbol{u}}_k(\lambda) \equiv \begin{cases} (\alpha_k + \beta_k)\bar{u}_1(\lambda) + (\beta_k - 1)\bar{u}_2(\lambda) + \beta_k \bar{u}_3(\lambda) & \text{for } |\alpha_k| \le K_k \\ (\beta_k^* - 1)\bar{u}_1(\lambda) + (\alpha_k^* + \beta_k^*)\bar{u}_2(\lambda) + \beta_k^* \bar{u}_3(\lambda) & \text{for } |\alpha_k^*| < \dfrac{1}{K_k} \end{cases} \qquad (k = 1, 2, 3) \qquad \text{(C.1)}$$

and

$$u_{kA} \equiv \begin{cases} (\alpha_k + \beta_k)u_{1A} + (\beta_k - 1)u_{2A} + \beta_k u_{3A} = \alpha_k u_{1A} - u_{2A} + \beta_k & \text{for } |\alpha_k| \le K_k \\ (\beta_k^* - 1)u_{1A} + (\alpha_k^* + \beta_k^*)u_{2A} + \beta_k^* u_{3A} = \alpha_k^* u_{2A} - u_{1A} + \beta_k^* & \text{for } |\alpha_k^*| < \dfrac{1}{K_k} \end{cases} \quad (k = 1, 2, 3). \quad \text{(C.2)}$$

In terms of the above definitions the transformations $T_{\bar{u}}^{\bar{v}}$ and T_u^v of Appendix A now read:

Transformation of color-matching functions (linear):

$$T_{\bar{u}}^{\bar{v}}: \quad \bar{v}_k(\lambda) = \kappa \, \mathbf{U}_k^{\,V} \bar{u}_k(\lambda) \ , \quad \mathbf{U}_k^{\,V} \equiv \frac{v_{kN}}{u_{kN}} \ , \qquad \kappa \neq 0 \qquad (k = 1, 2, 3) \ . \quad \text{(C.3)}$$

Transformation of chromaticity coordinates (projective):

$$T_u^v: \quad v_{kQ} = \frac{\mathbf{U}_k^{\,V} u_{kQ}}{\sum_{n=1}^{3} \mathbf{U}_k^{\,V} u_{kQ}}, \quad \mathbf{U}_k^{\,V} \equiv \frac{v_{kN}}{u_{kN}} \qquad (k = 1, 2, 3) \ . \quad \text{(C.4)}$$

(N is a normalization stimulus whose chromaticity coordinates in the new representation satisfy $v_{kN} \neq 0 \quad (k = 1, 2, 3)$).

The derivation of the above formulae is given in the same paper[40] as the transformation equations in Appendix A.

Appendix D: Interpolation

In the present paper, spectral tristimulus values of monochromatic stimuli are interpolated by fitting third order polynomial curves between successive data points. Assuming that the original CMF's refer to primaries $\boldsymbol{U}_i \ (i = 1, 2, 3)$, and letting $\bar{u}_{i\lambda}$ $(i = 1, 2, 3)$ denote the spectral tristimulus values of a monochromatic stimulus of wavelength λ, the corresponding spectral chromaticity coordinates are derived by means of the definition formulae

$$u_{i\lambda} \equiv \frac{\bar{u}_{i\lambda}}{\sum_{l=1}^{3} \bar{u}_{l\lambda}} \qquad (i = 1, 2, 3) \ . \tag{D.1}$$

Spectral chromaticity coordinates v_{jQ} $(j = 1, 2, 3)$ referring to any other primaries V_j $(j = 1, 2, 3)$ are calculated by means of the above formulae together with the projective transformation given in Eq. (A.2). To emphasize that in these cases T_u^v transforms purely between sets of spectral chromaticity coordinates, the index Q is here replaced by λ.

If $\bar{u}_i(\lambda)$ $(i = 1, 2, 3)$ denotes the set of continuously interpolated CMF's, the corresponding continuous spectral chromaticity coordinate functions describing the spectrum locus are analogously defined by the equations

$$u_i(\lambda) \equiv \frac{\bar{u}_i(\lambda)}{\sum_{l=1}^{3} \bar{u}_l(\lambda)} \qquad (i = 1, 2, 3) \ . \tag{D.2}$$

To create a set of continuously interpolated spectral chromaticity coordinate functions in a representation referring to new primaries V_j $(j = 1, 2, 3)$, the spectral chromaticity coordinate functions $u_i(\lambda)$ $(i = 1, 2, 3)$ defined above are transformed into new functions $v_j(\lambda)$ $(j = 1, 2, 3)$ by means of a projective transformation analogous to the one given in Appendix A — i.e., the transformation obtained by replacing the coordinates u_{iQ} $(i = 1, 2, 3)$ and v_{jQ} $(j=1, 2, 3)$ in Eq. (A.2) by the interpolation functions $u_i(\lambda)$ $(i = 1, 2, 3)$ and $v_j(\lambda)$ $(j=1, 2, 3)$, respectively.

Table 1. Chromaticity coordinates of the reference stimuli X', Y', Z' and R', G', B' as well as of the CIE Illuminant *E*, in the respective *XYZ* and *RGB* representations of the Judd-Vos modified 2° observer.

Stimulus	Chromaticity coordinates					
	XYZ representation			*RGB* representation		
	x'	y'	z'	r'	g'	b'
$\boldsymbol{X'}$	1	0	0	1.286778	-0.289693	0.002915
$\boldsymbol{Y'}$	0	1	0	-1.726122	2.754146	-0.028024
$\boldsymbol{Z'}$	0	0	1	-0.758220	0.129175	1.629045
$\boldsymbol{R'}$	0.730100*	0.269857*	0.000043*	1	0	0
$\boldsymbol{G'}$	0.275117*	0.716046*	0.008837*	0	1	0
$\boldsymbol{B'}$	0.169856*	0.017098*	0.813046*	0	0	1
$\boldsymbol{E}$	0.33499†	0.33618†	0.32883†	1/3	1/3	1/3

* Values obtained by interpolation of spectral chromaticity coordinate functions (see Appendix D).

† Values taken from Vos (Ref. 24).

Table 2. Chromaticity coordinates of the reference stimuli $\hat{R}^{\cdot}$, $\hat{G}^{\cdot}$, $\hat{B}^{\cdot}$; $R^{\cdot}$, $G^{\cdot}$, $B^{\cdot}$ and $X^{\cdot}$, $Y^{\cdot}$, $Z^{\cdot}$ as well as of the CIE Illuminant *E*, in the respective $\hat{R}\hat{G}\hat{B}$, *RGB* and *XYZ* representations of the Stiles-Burch$_{1955}$ 2° pilot group.

Stimulus	Chromaticity coordinates								
	$\hat{R}\hat{G}\hat{B}$ representation			*RGB* representation			*XYZ* representation		
	$\hat{r}^{\cdot}$	$\hat{g}^{\cdot}$	$\hat{b}^{\cdot}$	$r^{\cdot}$	$g^{\cdot}$	$b^{\cdot}$	$x^{\cdot}$	$y^{\cdot}$	$z^{\cdot}$
$\hat{R}^{\cdot}$	1	0	0	0.987276	0.013898	-0.001174	0.711098	0.288731	0.000171
$\hat{G}^{\cdot}$	0	1	0	-0.641980	1.603785	0.038195	0.140704	0.820029	0.039267
$\hat{B}^{\cdot}$	0	0	1	-0.016470	0.009406	1.007064	0.164841	0.023416	0.811743
$R^{\cdot}$	1.008820*	-0.009413*	0.000593*	1	0	0	0.719976	0.278331	0.001693
$G^{\cdot}$	0.379787*	0.628741*	-0.008528*	0	1	0	0.280003	0.709951	0.010046
$B^{\cdot}$	0.032081*	-0.016113*	0.984032*	0	0	1	0.168864	0.019861	0.811275
$X^{\cdot}$	1.219337	-0.223789	0.004452	1.307675	-0.309671	0.001996	1	0	0
$Y^{\cdot}$	-0.577170	1.609561	-0.032391	-1.827264	2.857460	-0.030196	0	1	0
$Z^{\cdot}$	-73.430328	8.968607	65.461721	-0.792535	0.136905	1.655630	0	0	1
E	0.579468‡	0.265210‡	0.155322‡	1/3	1/3	1/3	1/3	1/3	1/3

* Values obtained by interpolation of spectral chromaticity coordinate functions (see Appendix D).

‡ Values obtained by integration of color-matching functions (see Section 5).

REFERENCES AND NOTES

1. F. Viénot, Report of the activity of CIE TC 1-36 'Fundamental chromaticity diagram with physiologically significant axes', in *Proceedings of the Symposium '96 on Colour Standards for Image Technology*, Vienna, 1996 (Central Bureau of the CIE, Vienna, 1996), pp. 35-40.

2. The CIE committee TC 1-36 distinguishes between the "fundamental response curves", representing the fundamental spectral sensitivity functions of the three types of cones at the corneal level, and the "cone absorption curves" which are derived by correcting the fundamentals by the absorption of the lens and ocular media and the macular pigment. Hence, if $T_{media}(\lambda)$ denotes the spectral transmittance of the lens and ocular media and $T_{macula}(\lambda)$ denotes the spectral transmittance of the macular pigment, each cone absorption curve is given in terms of the corresponding fundamental response curve by the equation

$$\text{cone absorption curve} = \frac{\text{fundamental response curve}}{T_{media}(\lambda) * T_{macula}(\lambda)} .$$

3. CIE, *Proceedings of the 8th Session of the CIE*, Cambridge, 1931 (Cambridge U. Press, Cambridge, UK, 1932), pp. 19–29.

4. ISO/CIE, *CIE Standard Colorimetric Observers*, Publication ISO/CIE 10527 (Central Bureau of the CIE, Vienna, 1991).

5. W. S. Stiles and J. M. Burch, "NPL colour-matching investigation: final report (1958)," Opt. Acta **6**, 1–26 (1959).

6. R. Luther, "Aus dem Gebiet der Farbreizmetrik," Z. Tech. Phys. **8**, 540–558 (1927).

7. D. I. A. MacLeod and R. M. Boynton, "Chromaticity diagram showing cone excitation by stimuli of equal luminance," J. Opt. Soc. Am. **69**, 1183–1186 (1979).

8. R. M. Boynton, "A system of photometry and colorimetry based on cone excitation," Color Res. Appl. **11**, 244–252 (1986).

9. CIE, Draft 9 of CIE TC 1-36 "Fundamental chromaticity diagram with physiological axes," (Central Bureau of the CIE, Vienna, 1998).

10. W. S. Stiles and J. M. Burch, "Interim report to the Commission Internationale de l'Eclairage, Zürich, 1955, on the National Physical Laboratory's investigation of colour-matching," Opt. Acta **2**, 168–181 (1955).

11. J. H. Wold and A. Valberg, "Cones for colorimetry," in *Proceedings of the 23rd Session of the CIE*, New Delhi, 1995 (Central Bureau of the CIE, Vienna, 1995) Vol. 1, pp. 24–27.

12. T. Smith and J. Guild, "The C.I.E. colorimetric standards and their use," Trans. Opt. Soc. **33**, 73–134 (1931–1932).

13. H. S. Fairman, M. H. Brill and H. Hemmendinger, "How the CIE 1931 color-matching functions were derived from Wright-Guild data ," Color Res. Appl. **22**, 11–23 (1997).

14. D. B. Judd, "Reduction of data on mixture of color stimuli," Bur. Standards J. Res. **4**, 515–548 (1930).

15. D. L. MacAdam, *Color Measurement: Theme and Variations* (Springer-Verlag, Berlin, 1981).

16. The CIE *RGB* representation refers to the Wright primaries ***R***, ***G***, and ***B***, representing monochromatic stimuli of wavelengths 700.0, 546.1, and 435.8 nm, respectively (see Refs. 3 and 17). The norms of ***R***, ***G***, and ***B*** are defined so as to ensure that the chromaticity coordinates of Illuminant *E* are $r_E = g_E = b_E = \frac{1}{3}$.

17. W. D. Wright, "A re-determination of the trichromatic coefficients of the spectral colours," Trans. Opt. Soc. **30**, 141–164 (1928–1929).

18. E. Schrödinger, "Über das Verhältnis der Vierfarben- zur Dreifarbentheorie," Sitzungber. Kaiserl. Wien. Akad. Wiss. Math.-Naturwiss. Kl. **134**, Abt. IIa, 471–490 (1925).

19. CIE, *Proceedings of the 6th Session of the CIE*, Geneva, July 1924 (Cambridge U. Press, Cambridge, UK, 1926), pp. 67–70.

20. Other constraints have also been considered. For instance, D. Brainard (brainard@psych.ucsb.edu, personal communication, 1999) has suggested minimizing the difference between CMF's (Judd-Vos versus Stiles-Burch$_{1955}$) rather than between the spectrum loci of the chromaticity diagrams. This alternative seemed most attractive because of its simplicity. However, it turns out that such a minimization of differences of tristimulus values in three dimensions leads to

severe and considerable distortions of the chromaticity diagram (see Refs. 21 and 22). Yet another alternative would be to let the tristimulus vector to which the fundamental S response curve (S fundamental) refers serve as the *Z* primary. (See Section 9 for further details.)

21. J. H. Wold and A. Valberg, "A comparison of two principles for deriving *XYZ* tristimulus spaces," in *The 15th Symposium of the International Colour Vision Society,* Göttingen, July 1999. Abstract P40.

22. J. H. Wold and A. Valberg, "The derivation of *XYZ* tristimulus spaces: a comparison of two alternative methods," Color Res. Appl. (to be published).

23. D. B. Judd, "CIE Technical Committee No.7 "Colorimetry and Artificial Daylight," Report of Secretariat United States Committee," in *Proceedings of the 12th Session of the CIE,* Stockholm, 1951 (Bureau Central de la CIE, Paris, 1951), Vol. 1, part 7, pp. 1–60.

24. J. J. Vos, "Colorimetric and photometric properties of a 2^o fundamental observer," Color Res. Appl. **3**, 125–128 (1978).

25. S. L. Guth, J. V. Alexander, J. I. Chumbly, C. B. Gillman, and M. M. Patterson, "Factors affecting luminance additivity at threshold among normal and color-blind subjects and elaborations of a trichromatic-opponent colors theory," Vision Res. **8**, 913–928 (1968).

26. V. C. Smith and J. Pokorny, "Spectral sensitivity of the foveal cone photopigments between 400 and 500 nm," Vision Res. **15**, 161–171 (1975).

27. A. Eisner and D. I. A. MacLeod, "Blue-sensitive cones do not contribute to luminance," J. Opt. Soc. Am. **70**, 121–123 (1980).

28. W. Verdon and A. J. Adams, "Short-wavelength-sensitive cones do not contribute to mesopic luminosity," J. Opt. Soc. Am. A **4**, 91–95 (1987).

29. The contribution of the S cones to luminance has been somewhat contentious. Some authors claim that S cones do make a small contribution, whereas others maintain they do not. However, given that the contribution, if any, is minor, it is convenient to assume that the S cone contribution is zero. (See for instance A. Stockman and L. T. Sharpe, "Cone spectral sensitivities and color matching," in *Color vision: From Genes to Perception,* K. R. Gegenfurtner and L. T. Sharpe, eds. (Cambridge U. Press, Cambridge, UK, 1999), pp. 53-87.)

30. A. Stockman, D. I. A. MacLeod, and N. E. Johnson, "Spectral sensitivities of the human cones," J. Opt. Soc. Am. A **10**, 2491–2521 (1993).

31. G. Wyszecki and W. S. Stiles, *Color Science: Concepts and Methods, Quantitative Data and Formulae*, 2nd ed. (Wiley, New York, 1982).

32. CIE, *Colorimetry*, 2nd ed., Publication CIE No. 15.2 (Central Bureau of the CIE, Vienna, 1986).

33. F. W. Billmeyer, Jr. and H. S. Fairman, "CIE Method for Calculating Tristimulus Values," Color Res. Appl. **12**, 27–36 (1987).

34. In the paper by Stockman *et al.*[30], the proposed values are 0.68237 and 0.35235. If we apply these values, the maximum of $V^{\cdot}(\lambda)$ turns out to be 0.999777 (at 553 nm). To normalize $V^{\cdot}(\lambda)$ to a maximum value of 1.000000, the coefficients are multiplied by the factor $\frac{1}{0.999777}$.

35. O. Estévez, "On the fundamental data-base of normal and dichromatic color vision," Ph.D. dissertation (Amsterdam University, Krips Repro Meppel, Amsterdam, 1979).

36. The notation $expression|_{equation(s)}$ is to be understood as the result of initially performing the operation given in *expression* and subsequently making the substitution(s) indicated by *equation(s)*.

37. With the equations of the lines $L_1^{\cdot}$, $L_2^{\cdot}$, and $L_3^{\cdot}$ at hand, this result is of course more efficiently achieved by applying the alternative procedure outlined in Appendix C — i.e., by simply inserting the values of the coefficients $\alpha_k^{\cdot}$ $(k = 1, 2, 3)$ and $\beta_k^{\cdot}$ $(k = 1, 2, 3)$ [Eqs. (26), (28), and (36)] and chromaticity coordinates $r_{jE}^{\cdot}$ $(j = 1, 2, 3)$ and $x_{kE}^{\cdot}$ $(k = 1, 2, 3)$ [Eqs. (15) and (35)] into Eqs. (30). However, for the conformity of the presentation, the transformation equations used here for the more general derivations are those on the form of Eqs. (39).

38. CIE, *CIE 1988 2° Spectral Luminous Efficiency Function for Photopic Vision*, 1st ed., Publication CIE No. 86 (Central Bureau of the CIE, Vienna, 1990).

39. H. G. Sperling, "An experimental investigation of the relationship between colour mixture and luminous efficiency," in *Visual Problems of Colour* (Her Majesty's Stationery Office, London, 1958), Vol. 1, pp. 249–247.

40. J. H. Wold, "Colorimetric transformation equations allowing flexible normalization", Die Farbe (to be published).